СИБИРСКИЙ ФЕДЕРАЛЬНЫЙ УНИВЕРСИТЕТ
SIBERIAN FEDERAL UNIVERSITY

ГОД ОБРАЗОВАНИЯ В СОДРУЖЕСТВЕ НЕЗАВИСИМЫХ ГОСУДАРСТВ

# ПРОСПЕКТ СВОБОДНЫЙ-2016

МЕЖДУНАРОДНАЯ КОНФЕРЕНЦИЯ СТУДЕНТОВ,
АСПИРАНТОВ И МОЛОДЫХ УЧЁНЫХ

# ЭЛЕКТРОННЫЙ СБОРНИК МАТЕРИАЛОВ МЕЖДУНАРОДНОЙ КОНФЕРЕНЦИИ СТУДЕНТОВ, АСПИРАНТОВ И МОЛОДЫХ УЧЁНЫХ **«ПРОСПЕКТ СВОБОДНЫЙ-2016»**, ПОСВЯЩЁННОЙ ГОДУ ОБРАЗОВАНИЯ В СОДРУЖЕСТВЕ НЕЗАВИСИМЫХ ГОСУДАРСТВ

КРАСНОЯРСК, СИБИРСКИЙ ФЕДЕРАЛЬНЫЙ УНИВЕРСИТЕТ
15-25 АПРЕЛЯ 2016 Г.

Министерство образования и науки Российской федерации
ФГАОУ ВПО «Сибирский федеральный университет»

# Сборник материалов Международной конференции студентов, аспирантов и молодых учёных «Проспект Свободный-2016», посвящённой Году образования в Содружестве Независимых Государств

Красноярск, Сибирский федеральный университет, 15-25 апреля 2016 г.

Красноярск, 2016

# «Key Issues of Natural Sciences»

УДК 157.15, 631.453

# STUDY OF CHANGES IN SOIL PROFILE BY BIOLUMINESCENT ENZYME METHOD

**Baigina E.M., Shpedt A.A.**
**scientific supervisor Dr. of Biological sciences, Professor Kratasyuk V.A.**
**language consultant Ass. Prof. Belova E.N.**
*Siberian Federal University*

Environmental regulations in the land use become a priority due to the progressive anthropogenic load on soil and the requirements of sustainable development of territories. Modern productive, cost-effective methods of environmental assessment of different categories of land and informative comprehensive evaluation indicators are needed to rapidly solve problems in monitoring mode of modern land use [1].

Bioluminescent methods have high sensitivity to a variety of chemical compounds, typical for industrial discharges, pollutants in the soil, water, air (heavy metals, phenols, formaldehyde, pesticides etc.). The extinguishing level of bioluminescence is proportional to the concentration of toxic substances. Special light-recording equipment - bioluminometer and chemiluminometer - allows measuring the luminescence intensity of the reagent before and after injection of an unknown toxicant in a sample of small volume (0.2-0.5 ml). Analysis time is typically less than a few minutes. In addition, the advantage of this method is the possibility to carry out the analysis in the field [2].

## Materials and Methods

*Soil samples*

Sod-podsol soils, gray-humus soils, humus with dispersed carbonate were chosen for the analysis. Two vertical full-profiles were laid on these soils. Vertical profile № 4-6 was laid on a hillside of southern exposure in an enclosed micro-depressions (56º04'40 "N and 92º40'15" E), the steepness of the slope at the site of vertical profile is 3-4º. The height hypsometric mark is 248 m above the sea level. The vertical profile was on the grassland with the meadow-steppe vegetation. There is a pronounced wind erosion. The soil belongs to the organic-accumulative branch. The soil is also defined as a low-power-gray humus, slightly humic, medium loam, strongly deflated, on light loam carbonate.

Vertical profile № 5-1 was laid on a flat disturbed lands of pine forest (56º22'34,27"N and 92º57'29,45"E). The height hypsometric mark is 274 m above the sea level. The tract presented recent (winter) deforestation. The agricultural technique and the works for the harvesting of wood disturb the soil surface. The soil belongs to the texture-differentiated branch. The soil is also defined as a soddy-podzolic typical, petty, slightly humic, medium loam, on sandy clay.

The soil names were taken from the classification, based on the substantive-genetic approach. All the soils are assigned to the postlithogenic trunk.

The soil samples were taken in the layers at the depth of 0-10, 10-20 cm, as well as from the middle of each genetic horizon. Preparation of soil samples comprised drying, grinding, sieving through a sieve of 1.0 mm and 0.25 mm.

*Soil preparation and analyses*

The humus content, pH of salt and water suspensions, movable nitrate nitrogen and phosphorus by Chirikov method were determined.

For the bioluminescent enzyme assay the aqueous extract of soil was prepared [3, 4]. For this purpose, the soil was dried to air-dry. To a weighed portion of soil the fivefold volume of distilled water was added. It was stirred on a mechanical shaker for 30 minutes.

The extract was then filtered through a paper filter and centrifuged («Eppendorf» centrifuge 5810 R, 10 min., 3500 rpm).

*Bioluminescent enzyme toxicity test*

The bioassay of soil extracts was performed using couple enzyme system NADH: FMN-oxidoreductase + luciferase. Pollution of the soil was determined by inhibiting enzymes luminescence when adding the aqueous extract of the soil. The degree of contamination of soil extracts was analyzed for the residual value of the luminescence intensity (T%), which was according to the formula:

$$T=I/I_o{}^x100\%,$$

where I and Io – maximum luminescence intensity of the sample and the control (distilled water) respectively. Wherein, if T>80% – the sample is not contaminated (permissible degree of contamination), 50%<T<80% – the sample is contaminated, T<50% – the sample is heavily polluted. Luminescence of enzymes was recorded on a luminometer («PromegaGloMax» 20/20 Luminometer, USA). The measurements were performed in triplicate.

**Results and Discussion**

The content of humus in the gray-humus and sod-podzol soil assessed as very low and low. This is due to land degradation because of manifestation of deflation and soil disturbance during harvesting (Table. 1). Humus content decreases rapidly with depth and disappears in the parent soil-forming rock. The mass of gray humus horizon in the pasture does not exceed 35 cm, and that in the forest makes just 20 cm. The gray-humus soil pH of the aqueous suspension was varied with depth, from alkaline to strongly alkaline. In the profile of sod-podzol soil, pH of saline suspension is acidic and strongly acidic. Elevated levels of nitrate nitrogen were recorded only in the upper horizon of the gray-humus of soil. With the depth it declined sharply. The soddy-podzol soil was characterized by very low nitrate content throughout the profile.

Table 1 – The properties of soils and the residual luminescence of gray-humus and sod-podzol soils

| Horizon, itscapacity, cm | Depthofsampling, cm | Humus, % | pHKCl | pHH2O | $N\text{-}NO_3$ mg / kg | $P_2O_5$ mg / 100g | T,% |
|---|---|---|---|---|---|---|---|
| P. 4-6. Organic-accumulativebranch. Low-power-grayhumus, slightlyhumous, mediumloam, stronglydeflated, onlightloamcarbonate. Grassland. | | | | | | | |
| AY, 0-35 | 10-14 | 1,50 | 6,80 | 7,55 | 14,3 | 10,8 | 51,75 |
| | 23-27 | 1,24 | 6,95 | 7,80 | 13,3 | 2,8 | 57,72 |
| BCA, 35-103 | 55-60 | 0,31 | - | 8,30 | 2,2 | 10,7 | 96,19 |
| | 94-98 | 0,21 | - | 8,92 | 6,2 | 2,0 | 94,22 |
| Cca, 103-123 | 108-112 | 0,00 | - | 8,40 | 3,0 | 4,3 | 121,34 |
| P. 5-1. Texture-differentiatedbranch. Soddy-podzoltypical, petty, slightlyhumous, mediumloam, onsandyclay. Deforestationin a pineforest. | | | | | | | |
| AY, 0-22 | 0-10 | - | - | - | - | - | 28,97 |
| | 10-20 | 2,41 | 5,00 | 5,90 | 2,9 | 12,5 | 54,06 |
| EL, 22-44 | 25-35 | 0,55 | 4,40 | 5,60 | 1,8 | 11,8 | 77,06 |
| BT, 44-144 | 50-60 | 0,64 | 3,70 | 5,40 | 1,8 | 6,0 | 76,78 |
| | 80-90 | 0,50 | 4,00 | 5,70 | 2,0 | 9,50 | 88,84 |
| | 120-130 | 0,36 | 4,25 | 6,20 | 1,8 | 16,5 | 101,39 |

The residual luminescence was greatly changed (by two-three times) down the soil profile. It is evident that the accumulation of all kinds of pollution most strongly occurs in the upper layers; therefore, from the depth of about 55-80 cm soil contamination was not traced. The genesis of soils represented is different; however, the value of T behaves almost identically, which implies the universality of index. A positive, close relationship between the magnitude of the residual glow and depth of taking soil samples was detected (Table. 2). Relationship between the magnitude of the residual luminescence and the humus content and pH of the saline suspension was cramped and reverse. Accumulative properties of humic substances, despite their low maintenance, and quite pronounced alkalinity contributed to the contamination of soil surfaces. Dependencies between the value of T and the pH of the aqueous suspension and the content of mobile nutrients were unreliable.

Table2 – The relationships between the value of the residual luminescence and soil properties.

| Properties of soil | n | T,% | |
|---|---|---|---|
| | | r±Sr | $r^2$ |
| Depthofsampling | 20 | 0,82 ± 0,14 | 0,67 |
| Humus | 20 | - 0,71 ± 0,17 | 0,50 |
| $pH_{KCl}$ | 13 | - 0,72 ± 0,21 | 0,52 |
| $pH_{H2O}$ | 19 | 0,17 ± 0,24 | 0,03 |
| $N\text{-}NO_3$ | 19 | - 0,23 ± 0,24 | 0,05 |
| $P_2O_5$ | 19 | - 0,32 ± 0,23 | 0,10 |

Note: n – size of the sample; r ± Sr – the linear correlation coefficient and its error; $r^2$ – coefficient of determination. Authentically at n – 2 = 18 critical $r_{05}$ = 0,44; at n – 2 = 11 critical $r_{05}$ = 0,55.

The proposed bioluminescent express analysis for assessing the degree of soil contamination can be used by the Centers of laboratory analysis of Rosprirodnadzor, the Rosselkhoznadzor Reference Center, the National Center for stations and agrochemical service for conducting the state ecological, integrated monitoring and the protection of soil and land of different categories.

This work is supported by the project "Simple bioluminescence assay for determination of soil contamination in Krasnoyarsk Territory" of the Krasnoyarsk Regional Fund for Support of Science and Scientific-Technical Activity.

## References

1. Terekhova, VA Biotesting soils: Approaches and Challenges / VA Terekhova // Soil science. - 2011. - №. 2. - P. 190-198.

2. Kratasyuk, V.A. Principle of luciferase biotesting / V.A. Kratasyuk // In: Proceeding of the First International School "Biological Luminescence", Wroclaw, Poland, June 20-23, 1989, World Scientific Publishing Co.,- 1990, Singapore, New Jersey, London, Hong Kong, - P.550-558.

3. Soils. Methods of sampling and sample preparation for chemical, bacteriological, helminthological analysis. Interstate standards. GOST 17.4.4.02-84 - 2008. - Enter. 1986-01-01. - M .: Standartinform, 2008. - 8.

4. Soils. Sample selection. Interstate standards. GOST 28168-89 - 2008 - Introduced. 04/01/1990. - M .:Standartinform, 2008. - 7.

UDC 66.067.8.081.3

# WASTEWATER TREATMENT AT KRASNOYARSK KRAI REFINERIES USINGIONEXCHANGERESINPUROLITES950

**Dorohin A.S., Lipaikin S.J.**
**scientific adviserPhDin linguisticsMuchkinaE.S.**
*Siberian Federal University*

The development of various treatment methods for wastewater oil refineries produce is considered to be a most important challenge chemists face all over the world and, especially, in Russia. Various organic substances, as well as heavy metal salts, make this kind of waste extremely toxic.

Apparently, one of the metals found in wastewater is copper. However, this metal is a valuable industrial raw material as it has a wide range of applications: from electrical engineering to agro-industry (used as $Cu^{2+}$).

Human exposure to copper can cause serious health problems.Acute symptoms of copper poisoning by ingestion include vomiting, hematemesis and coma.In addition, copper is a neurotoxic heavy metal as well as mercury and lead[1].

Therefore, it's necessary todevelop breakthrough wastewater treatment systems and technologies which could be applied for getting copper out of industrial wastewater.

There are a number of methods of purification industrial waste from copper salts. However, only few of them allow manufacturersto recover this metal to be used in industry. One of the methods ision exchange.

Ion exchangers are usually water-insoluble solid substances which can take up ions of positive or negative charge from an electrolyte solution and release other ions of like charge into the solution in an equivalent amount. According to the charge of the ions exchanged ion exchangers can be classified as cation or anion exchangers. The so-called amphoteric ion exchangers can exchange both negatively and positively charged ions. Ion-exchange processes — apart from special cases — are reversible, i.e. they can be reversed by suitably changing the concentrations of ions in a solution[2].

As ion exchangers are water-insoluble substances they can be used advantageously for changing the ion composition of solutions without introducing further unwelcome ions or substances. They form a separate phase and can therefore be easily separated from solutions[2].

The main properties of ion exchangers are as follows[3]:

1. They have a high capacity which means that the number of exchangeable ions per unit weight of resin is high;
2. They retain their capacity (their ion-exchange property) even after long use;
3. They have a hydrophilic gel structure. This ensures good accessibility of functional groups and a better rate of diffusion of ions inside the resin particles;
4. They have good resistance, both in chemical and mechanical respects. They are neither dissolved in non-oxidizing acids nor in dilute alkali solutions, even at higher temperatures;
5. They do not dissolve in water even on being in long contact with it;
6. They operate rapidly, i.e. equilibrium is rapidly reached.

Ion exchange is one of the most effective treatment methods for liquid industrial waste. The ion exchange process is very effective at transferring the toxiccontent of a large volume of liquid into a small volume of solid.Selective ion exchange resins can reduce the concentration of metals in solutions to nearly zero[3].

The purpose of the experiment is to examine the exchange cation $Cu^{2+}$ capacity of Purolite S950, i.e. the ability and effectiveness of this ion exchanger to absorb copper.Previously carried out researches focused mainly on calculating resin capacity for calcium, but we assume that it can also absorb copper effectively: reaction centers of studied resin (aminophosphate functional groups) are soft bases, according to the principle HSAB, AFGa form stronger bonds with $Cu^{2+}$, than with $Ca^{2+}$[4].

Copper recovered in the process of desorption can be used in various fields of industry. The metal is mainly used for producing electrical wiring, including the windings of electromagnets, transformers and motors. Only silver has a better electrical conductivity at room temperature, but it is too expensive to be used for domestic wiring. Copper is both unreactive and easy to work with – it can readily be cut with a steel blade, and beaten, bent or soldered – which is why it is a good choice for use in pipework for water and gas supplies and heating systems. Altogether, a typical modern apartment contains around 200 kilograms of copper and a typical car - about 20 kilograms.

Copper-rich alloys are being used increasingly on surfaces in hospitals and schools, because copper has a proven antimicrobial action. Many pathogenic bacteria, viruses and fungi can survive for days or even weeks on various surfaces, but they are killed or deactivated within a matter of hours on copper surfaces. In tests, infection rates in hospitals have been greatly reduced. Copper alloys are also commonly used to make netting in fish farms; the copper prevents the accumulation of plants, algae and microorganisms, and improves the health of the fish as a result [5].

When carrying out the research we worked in the laboratories of the Siberian Federal University. The analysis was carried out at the Department of Physical and Inorganic Chemistry.

In the practical part of our research we dwelt uponthe resin capacity. Firstly, wecalculated the concentration of copper in the industrial wastewater and its pH, which was 2,9 mol/Land9,46,respectively. After that, we prepared the model solution which had the same characteristics.

Furtherwetestedthesorbingpropertiesoftheionexchangerandcomparedthemwiththeresultswehadgotforthemodelsolution.Thecalculationsandobservationsmadeitpossibletoconclude that the excess amount of the ion exchanger (1,5:1) completely absorbed copper from the wastewater solution.

The important advantage of this method is that ion exchange resins are environmentally-friendly.Moreover, a significant feature of this method is that the ion exchange resin can be used over and over again and it makes it possible to considerably reduce industrial production costs[3]. We hope this treatment method will be widely used by oil refineries in Krasnoyarsk Krai in the future.

**References**


1. Casarett & Doull's Toxicology, The Basic Science of Poisons, Fifth Edition [Internet resource]. URL: http://bookre.org/reader?file=514491&pg=1
2. Application of Ion Exchange Processes for the Treatment of Radioactive Waste and Management of Spent Ion Exchangers[Internet resource]. URL: http://www-pub.iaea.org/MTCD/publications/PDF/TRS408_scr.pdf
3. Fundamentals of Ion Exchange [Internet resource]. URL: http://desal.co.uk/pdfs/Technical%20Info/Dowex_-_Fundamentals_of_Ion_Exchange.pdf
4. ReutovO. Organic chemistryP.1 [Internet resource]. URL: http://bookree.org/reader?file=635362
5. Book of the elements [Internet resource]. URL: http://www.slideshare.net/sarikartini/howit-worksbookoftheelements-iisk

UDK544.137

# QUANTUM-CHEMICAL RESEARCH OF ENDOHEDRAL YTTRIUM-FULLERENES

**Kholtobina A. S.**
**scientific supervisor candidate of physical -mathematical sciences Kuzubov A. A.**
**language supervisor candidate of philological sciences Belova E. N.**
*Siberian Federal University*

Endohedral fullerenes are an interesting class of fullerenes because electron transfer from encaged metal atom to carbon cage has been known to occur and this oftentimes alters the electronic and magnetic properties of the fullerenes [1]. Particularly, endohedral yttrium-fullerenes have been obtained by several research groups [2-3].

The structural and electronic properties of endohedral yttrium-fullerenes were investigated using software package Openmx(Open source package for Material eXplorer), designed for nano-scale material simulations based on density functional theories (DFT) [4], norm-conserving pseudopotentials [5-6], and pseudo-atomic localized basis functions [7-8]. Simulations of single complex of $Y@C_{82}$, structure, consisting of two complexes of $Y@C_{82}$, and crystal of $Y@C_{82}$(face centeredcubic cell with a=11.457Å)[9]were performed. Since a fullerene molecule has pillow-like shape, an yttrium atom occupies several unequal states into fullerene cavity.

All these states, namely high, low1 and low2, that mean the top part of molecule, left and right on the bottom part of molecule, respectively, were investigated (see figure 1B). It was found, both low states have the lowest bond energies (-5.154 and 5.152 eV, respectively), which were calculated by using formula 1, and it indicates their equivalence, while bond energy for state high is -4.788 eV.Moreover,the dipole moment was calculated for systems high and low (2.638 and 2.859 D, respectively).

$E_{bond}=E_{comlex}- E_{ful}-E_Y$, (1)

where $E_{comlex}$–total energy of endohedral yttrium-fullereneY@C82, $E_{ful}$ - total energy of fullerene, $E_Y$ -energy of yttrium atom.

$$P = \frac{e^{-\frac{\Delta_i}{kT}}}{\sum_i e^{-\frac{\Delta_i}{kT}}}, \quad (2)$$

where $\Delta_i$ - difference between total energies of endohedral yttrium-fullerene Y@C82 with distinct states of yttrium atom.

The population probabilities, calculated by using formula 1, are $2.6\text{-}10^{-7}$ and ~ 0.5 for high and low, respectively. Sincethe population probability high is short, the polarizabilityof the system will be defined by the dipole moment of low state.

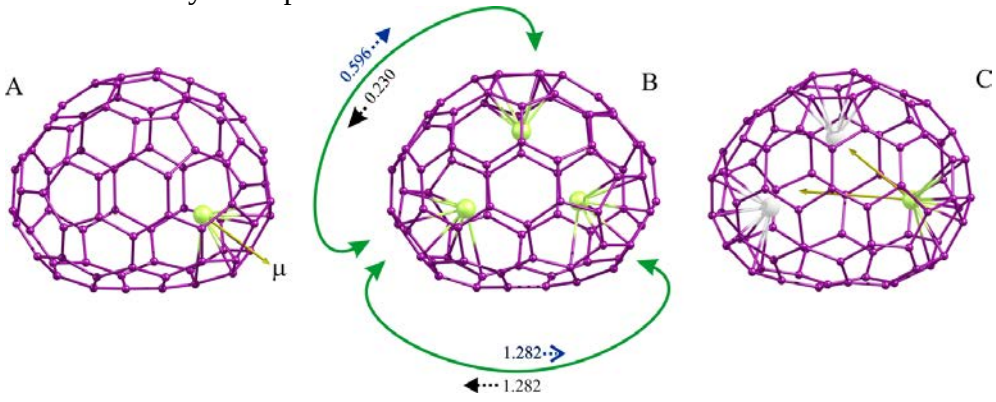


***Fig. 1 – A Direction of the dipole moment for state low, B transitions of yttrium atom between states high-low, low-high, low-low; C directions of the applied field***

Furthermore, the yttrium atom transitionbarriers between all potential states, namely from high to low, from low to high, from low1 to low2, were studied and values of barriers are 0.230, 0.596 and 1.282 eV, respectively. Consequently, it is more possible, that yttrium atom transition will be performed from state high to low along 111direction in crystal.

Simulation of endohedral yttrium-fullerenes with all potential states of yttrium atom, signed as high1-high2 (h1h2), low1right-high2 (l1rh2), low1right- low2left (l1r_l2l), low1left-low2right (l1l_l2r), low1left- low2left (l1l_l2l), were performed for the structure, consisting of two complexes of $Y@C_{82}$, which are arranged as in crystal (see Fig. 2). Among all researched structures the lowest bond energy was found for l1r_l2l geometry (-5.186 eV). Figure 2 indicates the barriers of all potential transitions of yttrium atom in these structures.

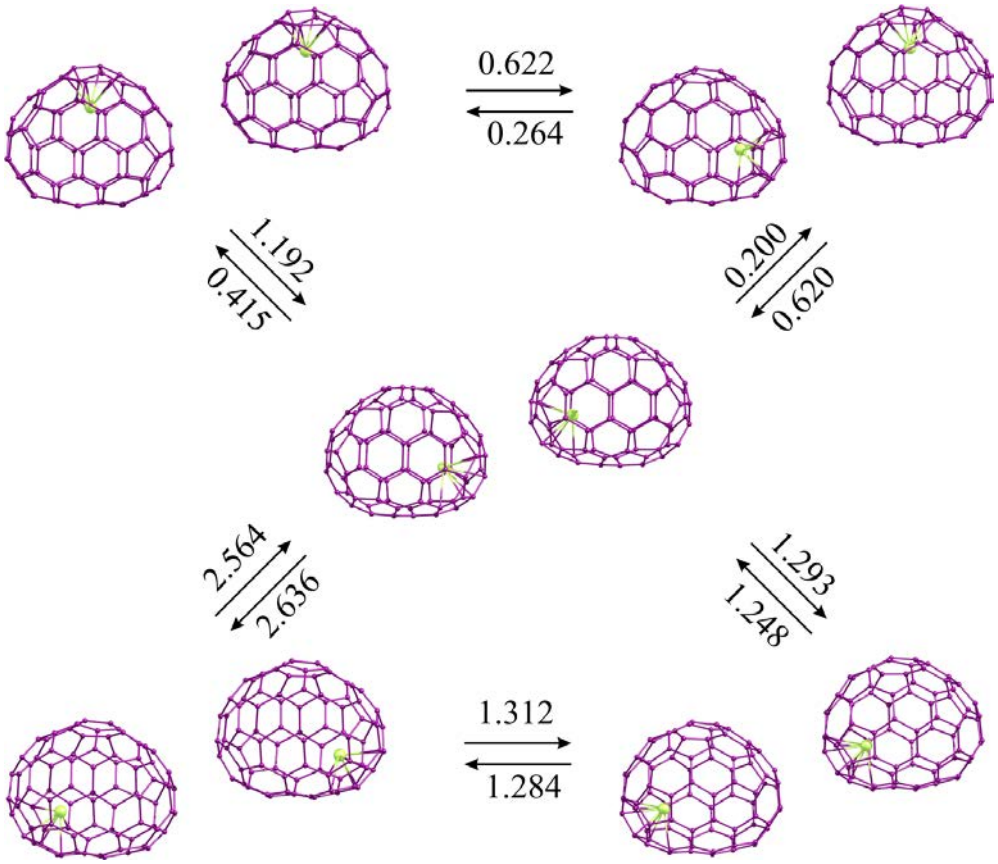


***Fig. 2 – The barriers of yttrium atom transitions for structures consisting of two complexes of $Y@C_{82}$***

In addition, the dipole moment - electric field correlation was considered. Furthermore, the electric field was applied along two directions (see Fig. 1C), the first of them runs along the transition from state high to one low, and the second one – along the dipole moment direction.It was found, the first and the second directionscorrespond to the complex and linear dependences (see Fig. 3).

Table 1 -The metal bond energies, the bond energies of molecule couple and yttrium atom charges for structures consisting of twocomplexes of $Y@C_{82}$

| Structure | $E_{bond\_Me}$, eV | $E_{bond\_2mol}$, eV | Charge of atom Y, a. u. |
|---|---|---|---|
| h1h2 | -4.800 | -0.034 | 0.428 |
| l1r_h2 | -5.007 | -0.083 | 0.307 |
| l1r_l2l | -5.186 | -0.076 | 0.305 |
| l1l_l2r | -5.155 | -0.012 | 0.307 |
| l1l_l2l | -5.158 | -0.017 | 0.304 |

The bond energies, the bond energies of molecule couple (the analogue of crystal lattice energy for structures, consisting of two complexes of $Y@C_{82}$) (see table 1)show that the lowestmetal bond energy belongs to the geometry with low states of yttrium atom as in case of single molecule. Obviously, the yttrium atom charge insignificantly changes, so only displacement of yttrium atom influences on the dipole moment.

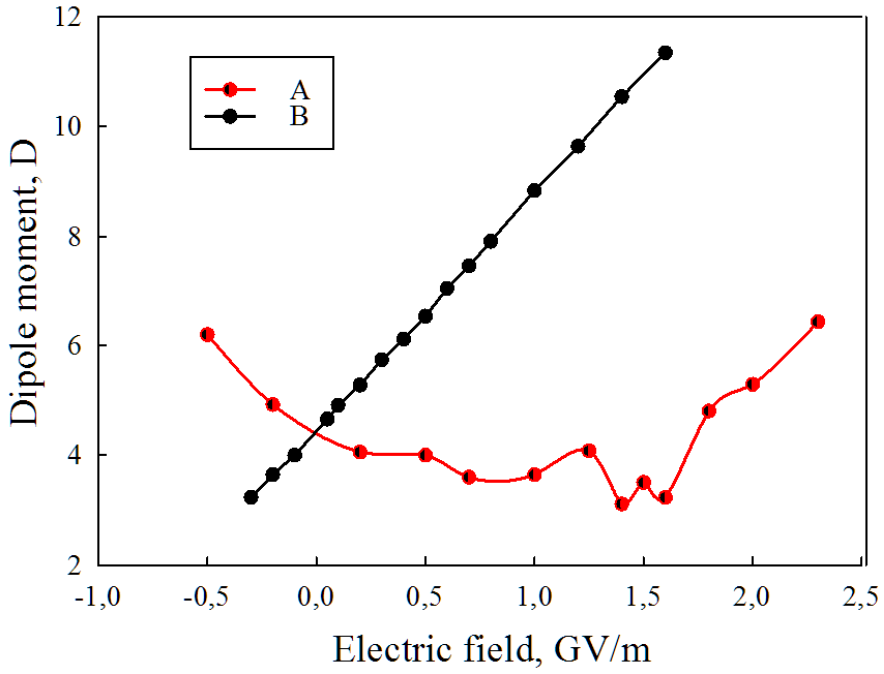


***Fig. 3 - The dipole moment - electric field correlation***

***A for electric fieldapplied along the transition from state high to low, B for electric field applied along the dipole moment direction***

Moreover, the calculations, connected with crystal structure of endohedral yttrium-fullerenes, were executed by analogy with the previous one. In particular, different states of yttrium atom (high, low1, and low2) were investigated and, it was found, that the most advantageous yttrium atom state is low (see Table 2). In addition, the crystal lattice energies were calculated for all crystal structures using formula 3.

$E_{cryst\_lat}=E_{crystal}-nE_{complex}$,(3)
where$E_{crystal}$–totalenergyofcrystalmodel, n – number of molecules Y@C82 in crystal model, $E_{complex}$– total energy of Y@C82

Table 2 - The metal bond energies, the crystal lattice energy and yttrium atom charges for crystals of $Y@C_{82}$

| Structure | $E_{bond\_Me}$, eV | $E_{cryst}$, eV | Charge of atom Y, a. u. |
|---|---|---|---|
| high | -5.240 | -0.452 | 0.424 |
| low1 | -5.610 | -0.458 | 0.295 |
| low2 | -5.579 | -0.425 | 0.299 |

The research of transition barriers from state high to low (0.661 eV) and from low1 to low2 (1.229) has shown that they insignificantly differ from analog transition barriers in single molecules (see Fig. 1). It is interesting to note that in this case synchronous displacement of

yttrium atoms descents in all endohedral yttrium-fullerenes.Furthermore, the crystal model of $Y@C_{82}$comprises four endohedral yttrium-fullerenes, which are arranged as in the face-centered lattice. The displacement of one yttrium atom from state high to low was investigated in this model (see Fig. 4).

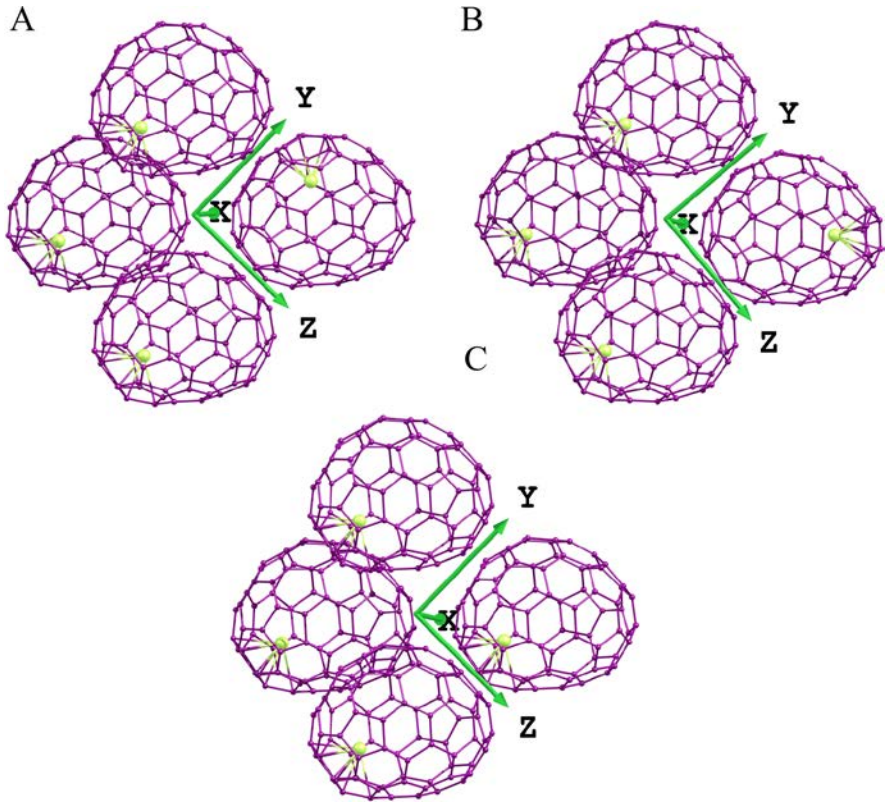


***Fig. 4 -The geometries of crystal model $Y@C_{82}$***
***A with high yttrium state, B with lowright yttrium state in one of the molecules, C with lowright yttrium state in each of the molecules***

In conclusion,endohedral yttrium-fullerenes$Y@C_{82}$simulations allow to form stable structures like $Y@C_{82}$, of both a single molecule and a crystal with ferroelectric properties. It can be applied inradiotronics and automatics and the development of piezoelectric devices, condensers and temperature gages.

**References**

1. S.Yung, C.-R. WangEndohedral Fullerenes: From Fundamentals to Applications, Word Scientific, 2014.
2. M. M. Ross, H. H. Nelson, J. H. Callahan, S. W. McElvany, J. Phys. Chem. 96, 5231, 1992
3. S. W. McElvany, J. Phys. Chem., 96, 4935, 1992.
4. P. Hohenberg, W. Kohn, Phys. Rev.,136, B864 1964.
5. G. B. Bachelet, D. R. Hamann, M. Schluter, Phys. Rev. B,26, 4199, 1982.
6. P. E. Blochl, Phys. Rev. B,41, 5414, 1990.
7. Morrison, D.M. Bylander, L. Kleinman, Phys. Rev. B,47, 6728, 1993.
8. T. Ozaki, H. Kino, Phys. Rev. B,69, 195113,2004.
9. 9. H. Suematsu, Y. Murakami, H. Kawata, Y. Fujii, N. Hamaya,O.Shimomura, K.Kikuchi, Y. Achiba, I. Ikemoto,Mat. Res. Soc. Symp. Proc., 349, 01994, 1994.

УДК 641.542.26=101

# FROM THE HISTORY OF THE FOUNDRY. TULA SAMOVARS

**Maslova N.V.**
**senior lecturer Shishova V.A.**
*Siberian Federal University*

If to speak about symbols of Russia, then one of them, of course, is the Tula samovar. Phrases the Russian samovar and the Tula samovar are inseparably linked with each other. It is already unclear what is more known to everybody. But the fact remains – the first high – volume output of samovars began in Tula thanks to what we can separate the Tula samovar from all samovar production.

History of the Tula samovar contains several centuries. There is a legend that it had been brought to Russia by Peter I, but actually it isn't true as the first mentions of the samovar appeared only in 1746 whereas Peter I died in 1725. It is still precisely unknown who had delivered a samovar to Russia, but such wonder interested Russians greatly. Soon special productions had been launched. As in those days they were done of copper or brass, it is no wonder that the first samples appeared in the Urals where metalproduction had been developed. But why is the samovar called "Tula"? Everything is very simple. For its production not only metal was necessary, but also people capable to process. In those days Tula was famous for the gunmen. It also became the reason that eventually samovars began to be produced in Tula. Besides the proximity to Moscow and St. Petersburg where the most part of production had been marketed, also promoted production movement exactly there.

In 1778 brothers Nazar and Ivan Lisitsyny made the first Tula samovar. 25 years later there was a samovar factory at which 26 people worked, and its turnover for those times was inconceivable – 1500 rubles. And in 25 years in Tula there were already 28 enterprises which made 120 000 copies annually.

Despite distinction in registration and finishing, the device of all samovars is identical. Each samovar consisted of the following parts: walls, jug, circle, neck, pallet, handles, repeyka, stebla of the crane, branch, bottom, lattice, dushnichka, subcones, wooden pridelok, rings and caps. It was difficult to get the craft of a samovarshchik. For a wall (case) a certain size of brass was cut, then it was curtailed into the cylinder, and this form was directed in twelve receptions. Brass was slightly cut with toothing from one side and then by blows of the hammer it was fixed on a connecting seam, after that it was delivered to the forge. Then the master (navodilshchik) repeated operations on seal of a seam by means of hammers and files and every time fixed by annealing in a forge. The son inherited the stock of a samovarshchik from the father, and in the process of wear it was replaced with the new one. The sum for acquisition of a tool kit varied greatly depending on chosen craft in production. For example, the set of the worker called “navodilshchik” cost 60 rubles. A few stoynas, files, scissors, forms for cutting metal, a gnedka and hammers were included in the package.

The main material for production of samovars were copper green (brass), red (alloy of copper of-50 - 63% and zinc of-37-50%), tombac (alloy of copper of-85-90% and zinc of-10-15%). Sometimes samovars were silvered, gilded, and even did of silver and cupronickel (an alloy of copper of-50 - 60%, zinc of-19-39% and nickel of-13-18%). Samovars from tombac had been manufactured 10 times more, than red ones (from an alloy of copper of-50-63% and zinc of-37-50%). Being more expensive, more beautiful, more magnificent, they went to rich and noble people. In 1850 the Tompakov samovar cost 25-30 rubles each, depending on finishing. But the bulk of samovars was produced from green copper. The production process of "the Tula miracle" consisted of 12 stages and was difficult and diverse. In the production

there was strict division of labor. There was hardly a case when the master would make completely all the samovar by himself .

Samovars and details to them were produced not only in Tula, but also in neighboring villages in a radius about 40 km from the city. So, the population of villages Lower Prisada, Hrushchevo, Banino, the Aspen Mountain, Badgers, Maslovo, Mikhalkov Desire the Tula county and villages, Torchkovo, Skorovarovo and Glinishcha of the Aleksinsky County from generation to generation specialized in the Samovar trade. Producing samovar walls, the master received raw materials from the manufacturer on weight, on weight also the samovar was given. The work was conducted in inhabited log huts all the year round except for summertime field works. The whole families had been busy with the Samovar manufacturing. Each samovarshchik for production of a samovar wall had his own the style. Circles, rings, pallets, caps and necks were most often produced cast - it was done by handicraftsmen-founders of the remains of copper and shot cartridges. In total such production has took 4-5 thousand handicraftsmen and a number of copper foundries. The highest rise of the Samovar production in Tula falls on the 1880th years. Due to the development of capitalism samovar factories arose in the form of a capitalist manufactory with civilian workers. Within centuries styles of samovars changed. By the end of the 19th century their number reached to 165. At such variety the production process can't be mechanized completely.. Therefore instruments of labor were almost invariable: kobylina in the form of iron bars with a thickening on the ends for forging of a samovar wall, weighing up to two poods everyone; stalls or a vertical kobylina for forging of smooth samovars, for a curve on samovars; gnedka for a razgranka of samovars; soldering irons for soldering of a jug with the samovar case; scissors for metal cutting; anvils; sets of hammers; a stamp for a branding of samovars; iron forms for formation of samovars.

A samovar was used not only at home, it was necessary while travelling and on festivities. For the same purpose travelling samovars were used. These samovars are unusual in a form, convenient in transportation (removable legs were screwed by screws, handles adjoined to a wall). In a form they many-sided, cubic, sometimes cylindrical. At the end of XIX - the beginning of the 20th century there appeared the new types of samovars - kerosene, a samovar of "Parichko" and copper samovars of Chernikov factory with the pipe device sideways. In the lattest the similar device strengthened the movement of air and promoted the fastest boiling of water. In 1977 there was launched a new combined type of the samovar. It represents the connection of a spherical and electric samovar, with a capacity of 5 liters. It can be boiled also by means of electricity, and charcoal, a splinter. Such sort of the samovar is convenient both at home and at the dacha, and outdoors.

## References


1. History of the Tula samovars. http://www.studfiles.ru/preview/1494687/
2. Cottage industry http://www.ya-zemlyak.ru/nps.asp?id=37

УДК 544.137

# ELECTRONIC AND MAGNETIC PROPERTIES OF TITANIUM PHOSPHIDE

**Melchakova J.A.**
**scientific adviser PhD Sc. (Phys.-Math.) Kuzubov A.A.**
**language adviser PhD in Linguistics Muchkina E.S.**
*Siberian Federal University*

There is a wide class of semiconducting materials which is characterised by the random substitution of a fraction of the original atoms by magnetic atoms. The materials are commonly known as semimagnetic semiconductors (SMSC) or diluted magnetic semiconductors (DMS). Dilute magnetic semiconductors are of great interest for fundamental science and applications as well as a great promise for spintronic applications of the future.

Spintronics is the new science of computers and memory chips that are based on electron spin rather than (or in addition to) the charge (used in electronics). Spintronics is an exciting field that holds promise to build faster and more efficient computers and other devices.

Understanding the source of ferromagnetism in dilute magnetic semiconductors has been a big problem slowing down their further development and application in spintronics.

The aim of this work is to research the peculiarities of the electronic structure of the new potential composite for this branch of science. Nowadays, the only material used as the basis of a computer transistor is silicon. Unfortunately, silicon supplies are being depleted and are likely to fail to meet the requirements of technology soon, so searching for alternative materials is our primary goal these days.

However, according to investigations of the nitrides of transition metals by Zhang et al. [1], the material properties of two-dimensional structures will differ from the bulk. So it is reasonable to suppose that new materials with unique electronic and magnetic properties could be found. Generally, we get an opportunity to investigate the properties of thin films which could be used in spintronics.

In this work the electronic and magnetic properties of TiP were explored. The basic hypothesis of the experiment was that the Fermi level of these materials was located in a band gap. Should the hypothesis be confirmed, TiP is to be considered a semiconductor.

**Methods and results**

Density functional theory as implemented in the Vienna Ab initio Simulation Package (VASP) [2] is used to calculate total energies.

The generalised gradient approximation with the Perdew, Burke, and Ernzerhof (PBE) [3] formalism was used to describe the electronic exchange and correlation. The Projector augmented-wave method together with a plane-wave basis with a cut-off energy of 400 eV was implemented. The Brillouin zone was sampled using the Monkhorst-Pack scheme [4], using a mesh of 2x2x1 for every structure. Convergence criteria for energies and forces were $10^{-5}$ eV and $10^{-3}$ eV*$A^{-1}$, respectively.

Firstly, a unit cell (UC) of titanium phosphide was optimized to get stable structures. Also, we calculated energy rates of a UC which allowed to calculate formation energy for two-dimensional structures.

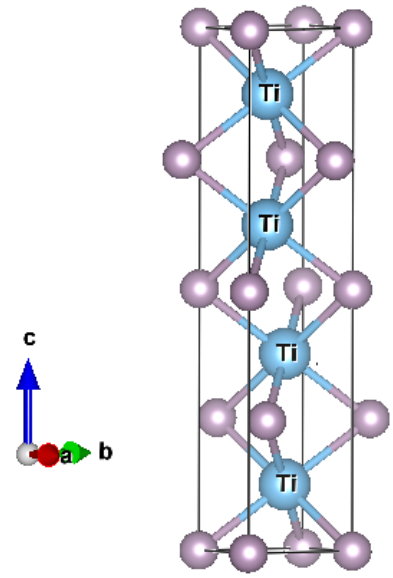


***Pic. 1 - The unitcell geometry of TiP***

Secondly, monolayers and bilayers were generated on the basis of the data we got while analyzing and constructing a unit cell. Thin films of TiP have different configurations and they depend on the positions of phosphorus atoms and titanium atoms: H (phosphorus atoms of two different layers are one above the other) and T (the phosphorus atoms in the second layer are deployed relative to the metal atoms at 60°).

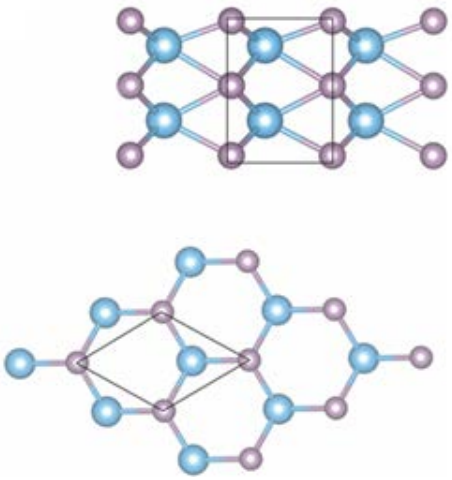

***Pic. 2 - T-configuration geometry***

Then we analyzed the electronic structure of 3d transition metals. The bandgap of about 0.5 eV was found to exist, thus, it is concluded that monolayers of titanium phosphide exhibit semiconducting properties.

To summarize, titanium phosphide is a semiconductor, so it can be used as a promising material for computer technologies and spintronics.

**References**

1. Zhang, S. Robust Ferromagnetism in monolayer Cronium nitride/ S. Zhang, Y. Li, T. Zhao and Q. Wang// SCI.Rep. – 2014. – Vol.4. – p.5241(7).
2. G. Kresse and J. Furthm Fuller, Phys. Rev. B 54 , 11169 (1996).
3. J. P. Perdew, K. Burke, and M. Ernzerhof, Phys. Rev. Lett. 77, 3865(1996)
4. H. J. Monkhorst and J. D. Pack,Phys. Rev. B 13, 5188(1976).

УДК 550.839

# MAPPING THE MORPHOLOGY OF SMALL PARTS BEFORE PRE - VENDIAN EROSION SURFACE USING A STRUCTURAL ATTRIBUTE OF THE SEISMIC WAVE FIELD

**Molodovskiy V.A.**
**scientific supervisor Professor Pozdnakov V.A.**
**language consultant Ass. Prof. Belova E.N.**
*Siberian Federal University*

The studied field is located in the Baikitpetroleum district which is proved to contain oil and gas in the Sinian complex. Riphean deposits, overlooking the pre-Vendian erosion surface, were exposed to denudation processes and chemical leaching that led to their satisfactory reservoir quality [2].

For the development of this field it is very important to get information on the morphology of the surface of the pre-Vendian as a promising interval along the surface of complicated erosional incision.

The need to analyze the spread of cuttings becomevivid when designing horizontal producing wells.

On drilling a well on a neighboring property in a promising range in the upper part of the carbonate Riphean complex, the horizontal trunk opened clastic deposits, represented by plastic clays. Having a total of 160 meters in the clays, the well again entered the Riphean carbonate strata. In the process of drillingclays, geological complications occurred manifested by intense absorption of drilling fluid [3].

Earlier in the time slices of the seismic cube isolated dendrite objects in the form of fiords and paleochannels were found. Clays opening interval was compared with the contours of the objects and it wasreported thatthe wellbore does pass through the zone previously determinedbythe seismic survey [3].

Processing and interpretation of seismic data 3D-CDP revealed the presence of the peculiar features of the wave pattern, resembling beds,channels and gullies by shape(Figure 1). These features clearly stand out against the background of the wave pattern, viewed in the range of pre-Vendian erosion surface. For the mapping of the identified bodies horizontal sections of the cubewere used as well as a structural attribute, reflecting the change in the wave pattern (Figure 2).

It should also be noted that the channels allocatedtemporary for the horizontal cross sections are confirmed in the vertical sections in the form of a temporary cube presented by peculiar cuttings (depressions) in the range of pre-Vendian erosional surface.

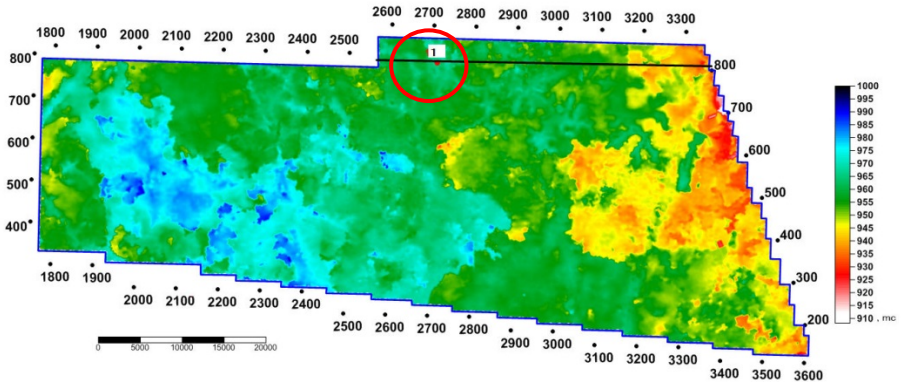


***a) - a fragment of the original cube cut***

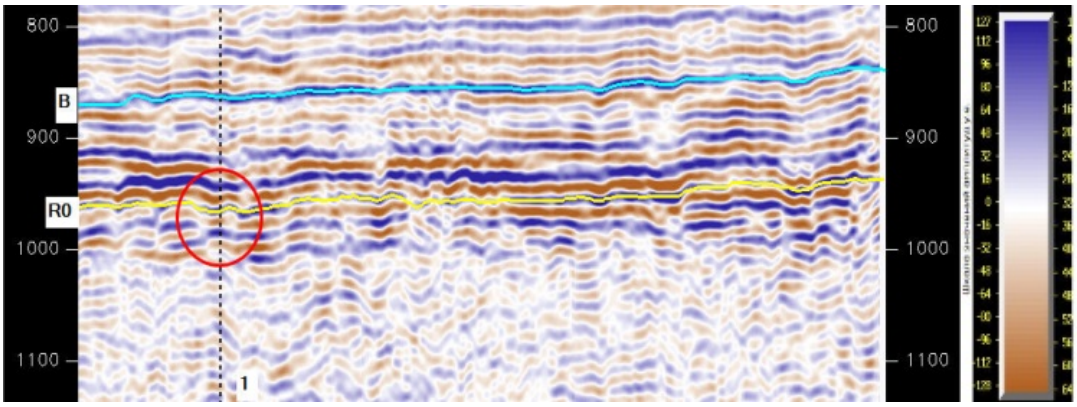


***b) - the time section along the borehole***

***Fig. 1 - Display of erosional incision in the horizontal (a) and vertical sections of the cube 3D***

As a result, the body mapped to mark the pre-Vendian surface, is defined as erosion incisions (Figure 3).

In the analysis of the well, trapped in the zone of distribution of cuttings, it is noted that within this range, there are clastic sediments of the VanavaraVendian suite. This fact allowed to assume that the erosion incisions are zones of spreading clastic sediments of the lower Venda and appeared during the pre-Vendian hiatus in sedimentation.

During the pre-Vendian hiatus vast amounts of Riphean strata and basement rockswere destroyed andtheclastic strata of the Lower Vendian wereformed from the destroyed rocks [1]. The bulk of erosional incision developed in the southern and south-western parts of the study area (Figure 1a).

Thus, it can be argued that the total immersion of the Pre-Vendian erosion surface in the south-west was complicated by erosional incision, which is reflected in its morphology.

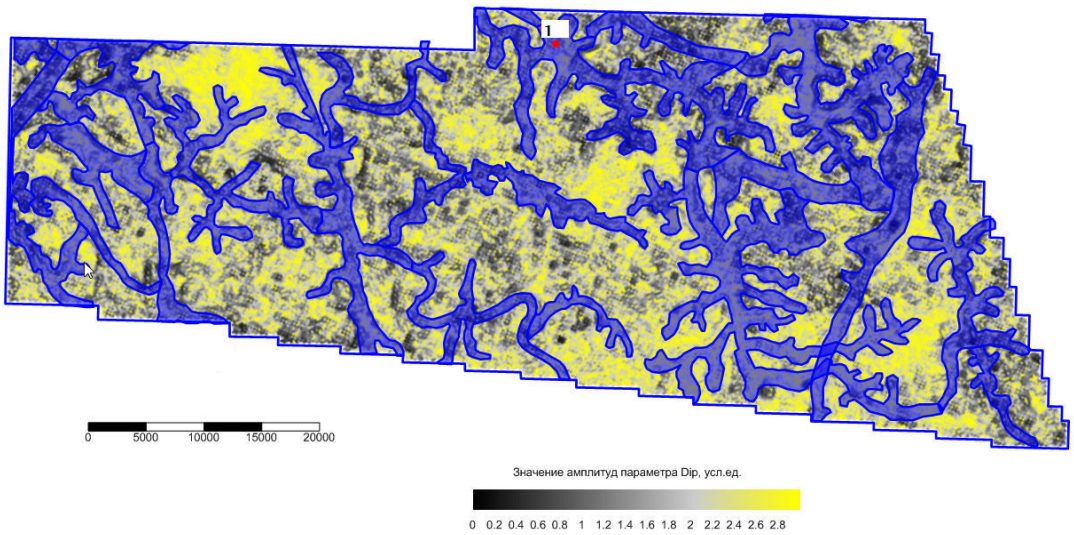


***Fig. 2 - Horizontal slice of the cube Dip in the range of the pre-Vendian erosion surface***

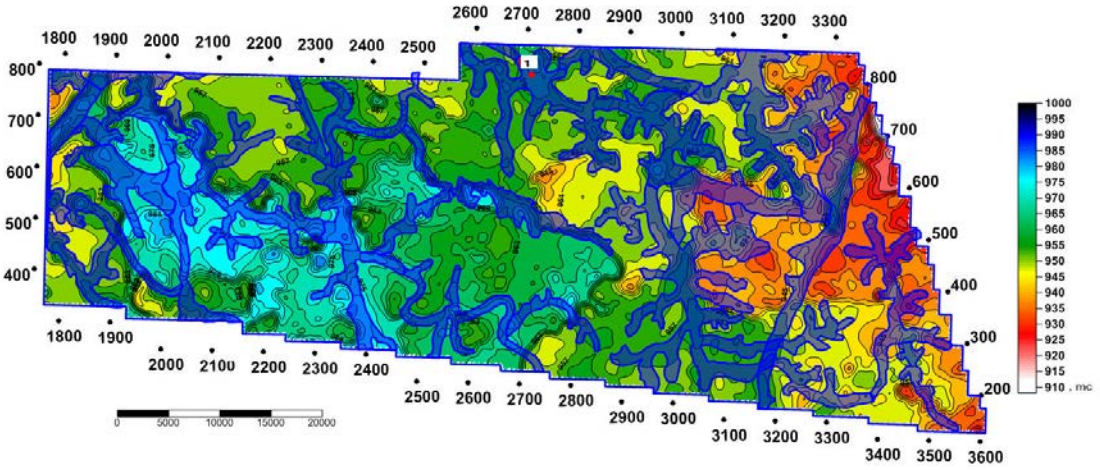


***Fig. 3 - Map of the isochronous pre-Vendian erosion surface***

The presence of incisionis also confirmed by time lag (Figure 1b).

Currently, the design of production wells is required to analyze their position in relation to the erosional incision bothin the vertical and horizontal sections of 3D cubes and a possible penetration by erosional incision direction of the barrel is adjusted.

1. Thestructural attribute of the seismic wave field has been identified, which allowedto more accurately distinguish fine details of the pre-Vendian erosion surface.

2. According to the materials of CDP-3D shooting mapping of the study area defined erosive cuttings, which in horizontal sections are shown in the form of beds, channels and gully-typebodies.

3. Considerationof erosional incisions in the design of horizontal wells helps avoid geological complications, associated with intense absorption in the intervals, containing the erosion incision,while drilling.

## References

1. Melnikov N.V. The Vend-Cambrian saliferous pool of the Siberian Platform (Stratigraphy, development history) /N.V. Melnikov; Min of nature.Resources, Sib. nauch.-research.Institute of Geology, Geophysics and Mineral Resources. - Novosibirsk: Publishing House of the SB RAS, 2009. - 148 p. (in Russian)

2. Harahinov V.V.Shlenkin S.I. Oil and gas Precambrian strata in Eastern Siberia by the example of theKuyumbinsko-Yurubcheno- Tokhomsky range of oil and gasaccumulation. - M .: Science World, 2011. - 420 p. (in Russian)

3. Tkachuk D.N. Thereport on processing and complex interpretation of materials of field seismic survey CMP 3D .. - M.: Krasnoyarsk, 2014. - 280 p. Funds of FSI "TFGI" in Krasnoyarsk Territory. (In Russian)

The paper discusses the structural features of the pre-Vendian erosion surface and dedicated erosional incision, which can create complications in the process of drilling.

УДК 665.6.035.6

# METHODS OF PREVENTING ARP DEPOSITS USING LOW-VISCOSITY MARINE FUEL AS A SOLVENT FOR HEAVY STILL BOTTOMS

**Nefedyeva T.N., Balaganskaya A.G.**
**scientific supervisor Lesyk E.I.,**
**language supervisor Stepanova T.Y.**
*Siberian Federal University*

Crude oil is a polyphase heterogenous system. When ambient conditions are changed the disengagement of high-molecular-weight oil components comes around. Such oil components are called asphaltene-resin-paraffin (ARP) deposits. They are considered as a very complicated dispersed system. Differences in the composition and the structure of the deposits set requirements to chemical reagents and particularly to the asphaltene-resin-paraffin deposits remover. The removers must have a balance between solvent ability and ability to break conglomerates of hardly-soluble components into small pieces. They have to keep this balance because it is a complicated task to select the solvents for all groups of hydrocarbons of oil deposits taking into account environmental requirements.[8]

The formation of these substances on the walls of oil storage units and pipelines considerably reduces the overall system performance and the running efficiency of pumping plant. The cleaning of the fuel storage tank is a process that should be done once in two years in case of the automobile gasoline storage, and twice in two years with lubricants, which contain dopants. Tanks for other oil-products which have similar physical and chemical properties are cleaned as needed, which is determined by the technical specifications of petroleum product storage facilities and the engineering status of the containers.[2]

Methods of preventing ARP deposits which are used nowadays don't allow to avoid their formation. So it is a urgent problem to remove the asphaltene-resin-paraffin deposits from the processing facilities.[4]

There are various methods of preventing ARP deposits such as physical methods (mechanical mixing, ultrasonic vibrations), thermal treatment (flushing with hot petrol or water as the coolant), chemical ones (solvents and removers).[3,5]

Taking into consideration the disadvantages of different solvents and removers, and using analytical and patent review, it was determined that solvents based on oil and oil-products are the most appropriate remover of ARP deposits. Apart from this, ARP deposits aren't an inevitable waste of petroleum industry, they could be involved in production of bitumen, naphtha residue, lubricants.[1]

The aim of this research is to explore the composition of the asphaltene-resin-paraffin deposits forming in the oil storage tanks at «Achinsk refinery of Eastern oil company, Limited», to select effective and affordable solvent, to determine the effect of injection of asphaltene-resin-paraffin deposits into the Burner Fuel 100 composition on the complex of technical and operational characteristics.

The subjects of the research were chosen benthal ARP deposits formed in the fuel storage tank, the burner fuel 100, low-ash fuel oil (State Standard 10585-2013), low-viscosity marine fuel (State Standard 32510-2013).

To select a hydrocarbon solvent for asphaltene-resin-paraffin deposits in the investigated product and naphtha oil, the content of the main group components (hydrocarbons + paraffin waxes, gums, asphaltenes) was identified. The hydrocarbon type content of the naphtha oil, the ARP deposits, was made by Markusson adsorption method. [6] The received data is given in Table 1.

Table 1 - The content of the group components of the ARP deposits and the naphtha oil in mass percents

| Type of oil-product | Hydrocarbons + paraffin waxes | Paraffin waxes | Gums | Asphaltenes | Mechanical impurities | Water |
|---|---|---|---|---|---|---|
| ARP deposits | 84,8 | 18,7 | 9,6 | 0,1 | 2,4 | 3,1 |
| Burner fuel 100 | 66,9 | 3,0 | 28,1 | 3.1 | 1,0 | 0,9 |
| Low-viscosity marine fuel | 99,1 | 2,8 | 0,9 | - | - | - |

It was diagnosed that the benthal ARP deposits are characterized by high content of lube oil and paraffin waxes.

Based upon the content of the group components low-viscosity marine fuel was offered as the solvent for ARP deposits. Low-viscosity marine fuel includes hydrocarbon compounds which contain alkane and aromatic structures, which are the closest to paraffinic oil substances of ARP deposits.[3]

The method for the orthogonal planning of experiment was used to determinate the influence of introduction ARP deposits with low-viscosity marine fuel as the solvent in burner fuel 100.

The content of the ARP deposits and the low-viscosity marine fuel in naphtha fuel varied in the range of 0-10 weight parts with the step 5 weight parts, provided the content of burner fuel 100 is a constant value - 100 weight parts.

The composition of mixtures and the experiment matrix are given in Table 2.

Table 2 - Split of oil products in samples

| Numeral order of the samples | | 1 | 2 | 3 | 4 | 5 | 6 | 7 | 8 | 9 |
|---|---|---|---|---|---|---|---|---|---|---|
| Characteristics of the analyzed mixture | Low-viscosity marine fuel | 0 | 0 | 0 | 5 | 5 | 5 | 10 | 10 | 10 |
| | ARP deposits | 0 | 5 | 10 | 0 | 5 | 10 | 0 | 5 | 10 |
| | Naphtha oil | 100 | | | | | | | | |

The mixtures were prepared at the temperature of 70 degrees Celsius. Firstly the ARP deposits were combined with the low-viscosity marine fuel until a homogeneous mixture was obtained and then the burner fuel 100 was added. The received samples were researched for compliance with the complex of technical and operational characteristics for burner fuel 100 (State Standard 10585-2013), thus were measured such parameters as freezing point (State Standard 20287-91), kinematic viscosity (State Standard 33-2000). All the experimental data was processed using TurboPascal program. Outline curves were constructed using Microsoft Excel 2007 program.

The task of this research was to designate an optimal quantity of low-viscosity marine fuel as a diluent of ARP deposits with due attention to passport requirements of naphtha fuel for freezing point, kinematic viscosity and to specify the costs of the raw materials of the experimental mixture counted up to the cost of burner fuel 100.

The method of the orthogonal matrixes makes it possible to get an approximate estimator of the beta coefficients and find a significant influence of the variable value on the properties of mixture, to find the solution of the questions, which appeared during the specification writing for the appropriate material.[7]

Using the method of the orthogonal planning of experiment, a graphic chart based on the freezing point change depending on the composition of the mixture was built. The ratios of ARP deposits and low-viscosity marine fuel were the variable values in this experiment. The outline curves for objective variables are shown in Figures 1 and 2.

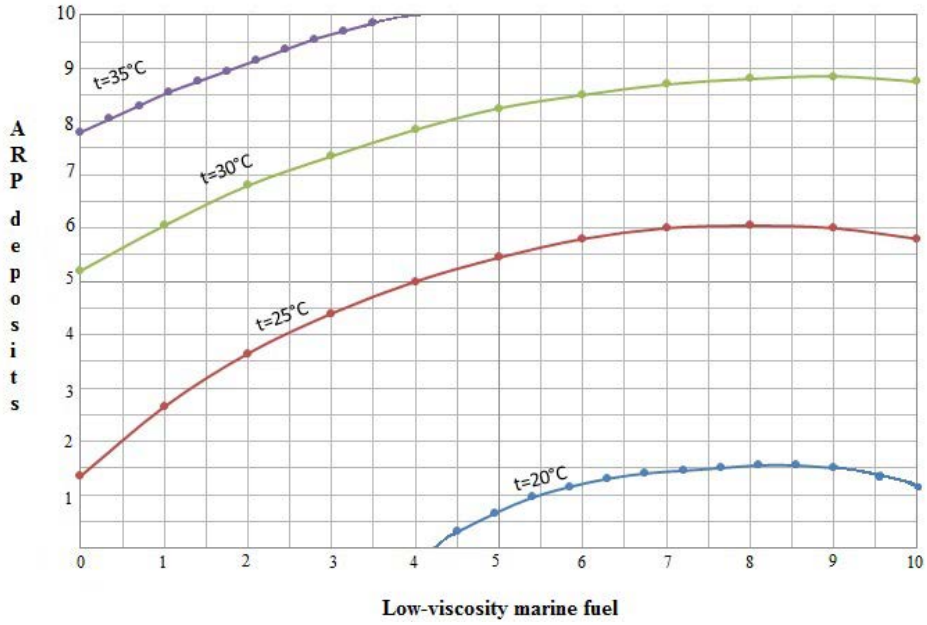


***Figure 1 - Influence of the ratios of ARP deposits and low-viscosity marine fuel on freezing point of the experimental mixtures***

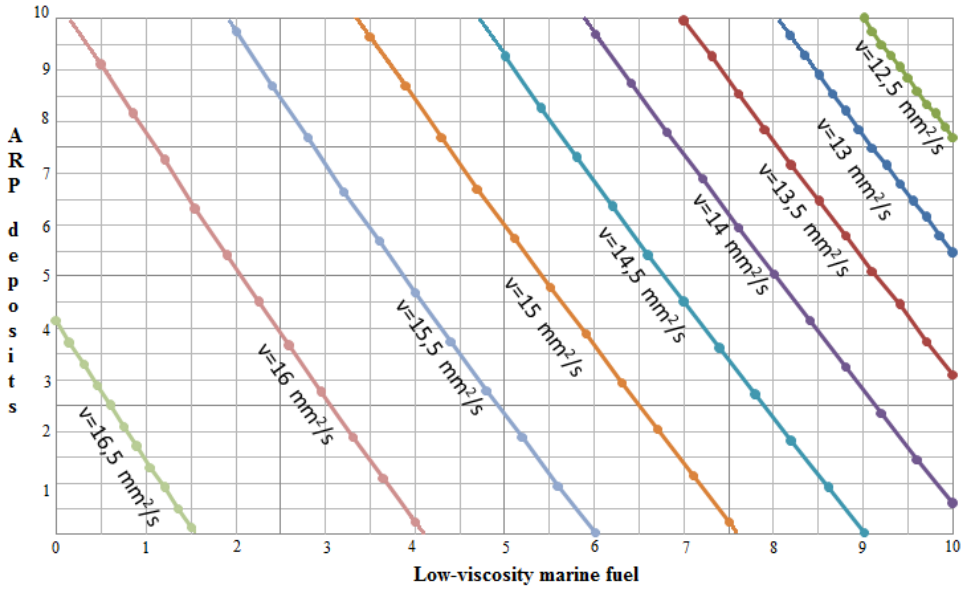


***Figure 1 - Influence of the ratios of ARP deposits and low-viscosity marine fuel on kinematic viscosity of the experimental mixtures***

Based on the made experiment it was specified that the optimal ratio of ARP deposits and low-viscosity marine fuel is in the range of (5÷6): (5÷6) for 100 weight parts of burner fuel 100. According to the obtained data it was diagnosed that the sample which contains 5:5:100 in the weight parts satisfies State Standard 10585-2013 for burner fuel 100.

For the implementation of the received mixture at «Achinsk refinery of Eastern oil company, Limited» the cost of the raw materials of the mixture is calculated for the commercial scale, accepting the condition that freezing point is 25 °C. In accord with the graphic chart it is assumed that the ratio of ARP deposits and low-viscosity marine fuel is 1:1.

It is set about mass ratio 5:5:100 (low-viscosity marine fuel : ARP deposits : naphtha fuel), in this case the percentage is 4,5:4,5:91. The low-viscosity marine fuel price is 17454 rouble/tonne, the naphtha fuel price is 6493 rouble/tonne, the APR deposits are free.

The next action is the recalculation for 1 tonne of the low-viscosity marine fuel (LVMF) and the ARP deposits (ARPD) at the weight ratio 1:1:20, in case the percentage is the same. These components are got involved into the naphtha fuel (NF) and as a result it is a mixture of 22 tonne. Then this mixture is sold at the price of the naphtha oil.

The raw material cost, excluding cleaning with the help of pumping machinery and other equipment, is calculated by the formula:

$$G_{ARPD} \cdot C_{ARPD} + G_{LVMF} \cdot C_{LVMF} + G_{naphtha\ oil} \cdot C_{naphtha\ oil} - G_{product} \cdot C_{product} = C' \quad (1)$$

where G – the mass of the component, tonne;

C – the cost of the component, rouble/tonne;

C'– the cost of the raw material of the experimental mixture counted up to the cost of burner fuel 100.

$$1 \cdot 0 + 1 \cdot 17454 + 20 \cdot 6493 - 22 \cdot 6493 = -4468 \text{ rouble/tonne.}$$

## References


1. Sunyaev Z.I., Safieva R.Z., Sunyaev R.Z. Oil dispersions. M .: Chemistry, 1990. 226 p.
2. Ivanova L.V. ARP deposits in the processes of recovering, transportation and storage / L.V. Ivanova, E.A. Burov, V.N. Koshelev // Electronic scientific journal "Oil and gas business." - 2011. - №1 - P. 268-270.
3. Kamenschikov F.A. Removing ARP deposits with solvents. M.: Izhevsk 2008
4. Bulatov A.I. Kusov G.V., Savienok O.V. Asphaltene and hydrate deposits: prevention and removal. Krasnodar Univ. The house "South", 2011. T. 2.
5. Dolomatov M.Y. and other. Physical and chemical bases of the directed selection of solvents asphaltene substances. Moscow, 1991.
6. Fisherman B.M. Analysis of oil and oil products. Moscow: State scientific and technical publishing house of the oil and mining and fuel literature. 1962, p 888
7. Evstratov V.F., Schwarz A.G. Experimental design and application of computer technology in the synthesis of rubber. Moscow: "Chemistry" Publishing House, 1970. 257 p.
8. Sharifulin A.V. Physical and chemical basis for the use of composite materials for intensification of oil production at the late stage of field development / A. V. Saifulin, A. F. Vildanov, I. A. Gur'yanov, V. S. Garifullin, Kazan, 2009. 10 p.

УДК 553.9

# EVALUATION OF THE RELIABILITY OF THE RESOURCE BASE IN THE «OC «ROSNEFT» IN THE IRKUTSK REGION

**Shatalov I.I.**
**Scientific adviser: principal project engineer Dadakin N.M.**
**language adviser Ass.Prof. Belova E.N.**
*Siberian Federal University*

The reliability of the resource base and hydrocarbon recovery rates based on the specification of the geological 2-D model of the area and the integration of the new techniques of probabilistic estimation of hydrocarbon has been evaluated with a view to the most effective and consistent implementation of geological exploration in the areas of licensed areas of «OC «Rosneft» in the Irkutsk region.

There was a need in complex revaluation of geological and geophysical information on the territory of exploration projects in licensed areas of «OC «Rosneft» in the Irkutsk region due to the increase in their number. This work aims to reduce technical and economic risks of geological exploration work and to determine the optimal path for the development of hydrocarbon potential of the region which is an urgent task for the company, the latter actively participating in the implementation of the existing programs aimed at increasing and reproduction of the mineral resource base of hydrocarbon raw materials. The results of the updated geological 2-D model covering the licensed areas of «OC «Rosneft» in the Irkutsk region, including the adjacent ones are presented in the work. The objects for further geological studies were justified while preparing the programme of exploration in the licensed areas based on the detailed regional geological 2-D model for all existing and prospective productive horizons. A new method of probabilistic estimation of the resource potential of the area was used to comprehensively assess the uncertainties in the calculated parameters that are present at the stage of exploration [2]. It should be noted that, the attempt to build sector models of the selected traps to determine the approximate to the realities of the recovery rate of oil and gas was made based on the results obtained. As a result, progress in testing will be published in future.

The integrated geological model reflecting the productive horizons was upgraded on the basis of the results obtained from the exploration of the territory of the Irkutsk region for the year of 2015. The results of drilling and testing wells with the preparation of stratigraphic top horizons were used including the exploration well D-67 drilled in 2015 .

Structural maps of the reflecting horizons were built in the course of work in the first place: A – the top of the osinsky horizon; B – the top of the tetersky suite; reflection horizon M2 – the top of nep suites; F - the surface of the foundation [1]. The method of "spine-approximation with invariant model of the field" was adopted as the technique to construct a method of "spine-approximation with invariant model of fields", which, as shown, is the best method for most types of maps.

Regional structural maps were taken as a bases and presented in the recent reports on local structures, maps of reflecting horizons referred to above were integrated in, as well as those of the top of the tetersky, sobinsk, khatanga, and nep suites and the top of the basement, derived from the interpretation of seismic data. Development of structural maps of the reflecting horizon M2 presented the greatest difficulty due to the presence of protrusions of the Foundation on the territory of the licensed areas. These projections were allocated according to the results of interpretation of seismic data 3D seismic acquisition and integrated in the structural map [3].

Structural maps of the top and base reservoirs were developed at the final stage and effective depth maps of strata for the reservoirs were presented, revealing the zones of absence of the collector. Layers B13 and B10-13 were the most difficult for the construction plans of sewers due to the small capacity of Reservoir B13 and its local manifestation in the southern part of the territory and the absence of B10-13 in the central part of the square.

The concept of allocation of volumetric objects "Sweat Areas" was taken in the development with regard to the trend of exploration works in the region to assess the credibility of the resource base. Its essence lies in the correlation of zones with improved FES with projections archean-early Proterozoic basement. Palaeotopography of projections served as a platform for the formation of a low-growth areas of algal mats.

Probabilistic estimation of geological and recoverable oil resources are based on the volumetric method, some or all, the choice of the expert, parameters of theestimation are presented as independent random variables. The total value of the inventory is treated as a function of these random parameters. The range of total values of stocks characterizes the uncertainty of reserves estimates and is characterized by the uncertainty of each volumetric parameter. The minimum, maximum and most probable value of the parameter and the type of probable distribution are defined (Figure 1) and set for each estimation parameter on the basis of available a priori information.

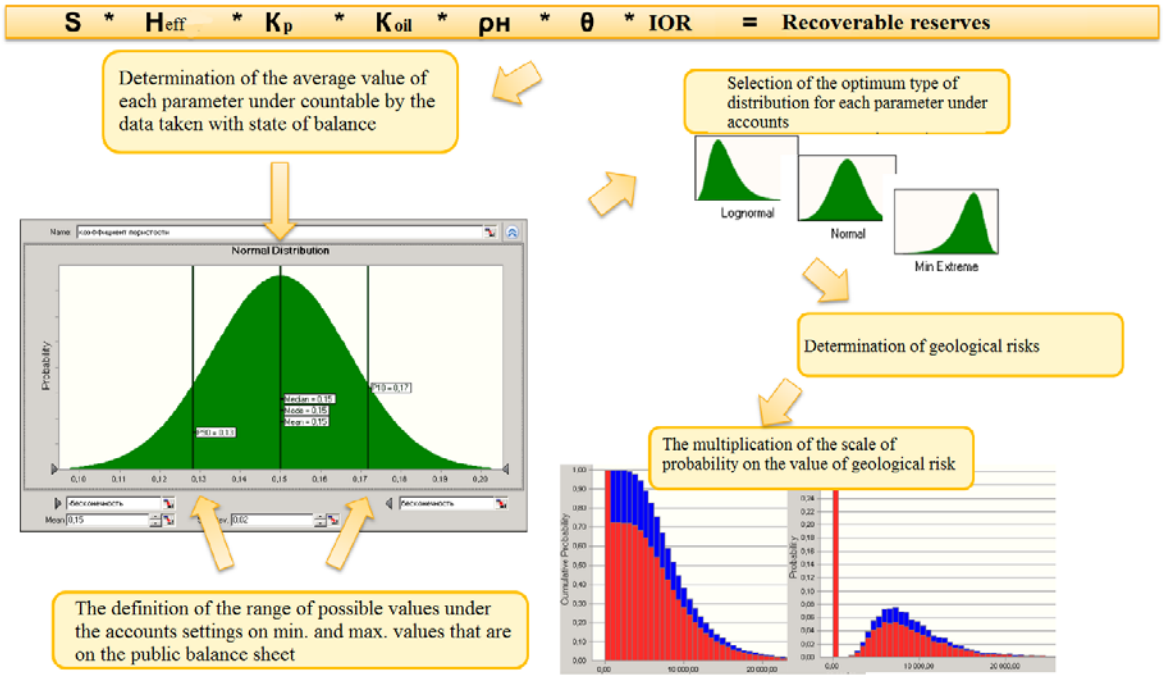


***Figure 1 - Description of resources counting by the probabilistic method***

Data of the state balance of resources of oil, gas and gas condensate fields of adjacent fields were taken as volumetric parameters. Also, the bulk of the available geological and geophysical information was analyzed. Maps of effective depths were taken as reliable estimations of the distribution of effective oil-saturated mass, because it allows to correctly specify the stochastic distribution of the mass parameter throughout the trap. The selection of productive strata on the basis of the analysis of the distribution of collectors areas was produced for all possible horizons. It should also be noted that the contour of the traps was not included in the calculation, but this circuit was part of the open field. As a result, the discrepancy between the obtained results and the approved resource potential areas has

emerged. The volume of resources calculated by means of the new method, was lower than that estimated earlier, therefore, there is a need to adjust the planned exploration on the site and determine priority sites (table 1).

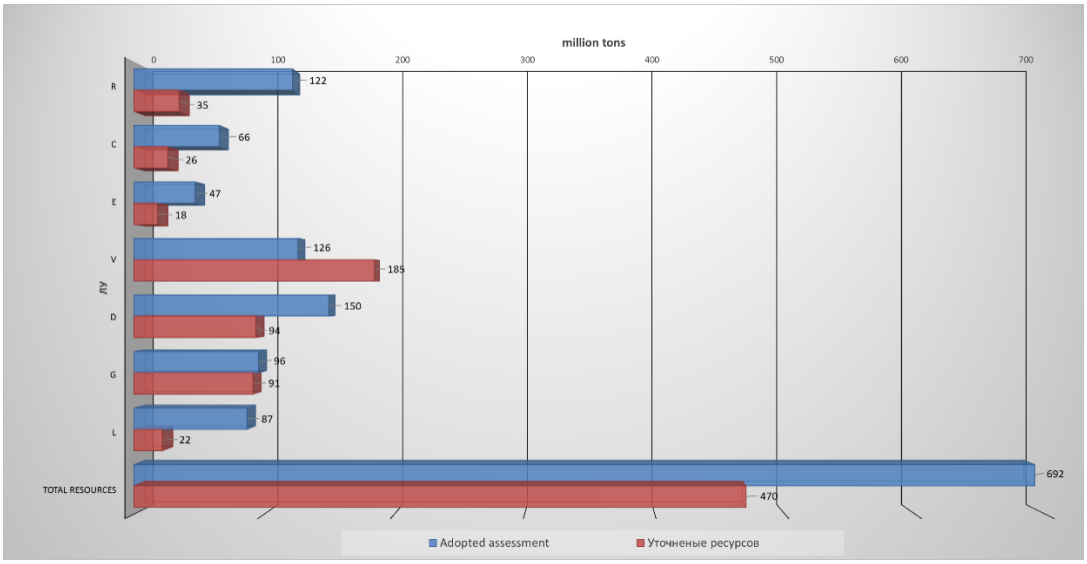


***Figure 2 - Comparative histogram of the current estimate and updated resource of Pmean oil category***

The new method to assess the resource potential of the plots was applied on the basis of an integrated resource development to identify the distribution of layers, and of collective probabilistic approach to select estimation parameters. As a result, the resource potential of the license areas was clarified in the set direction of exploration work development in the Company. Also recommendations are given on selecting priority sites of exploratory drilling. Thus, the most promising objects are: trap 1 and 3 V license areas, trap 1 D license areas, trap 3 G license areas.

It should also be noted that the average value of 0.21 is taken as the coefficient of oil extraction in the proposed resource potential and does not reflect the actual value varied according to geological and petrophysical properties of reservoir formations.

IOR stage is taken on the «invest Memorandum» by analogy with adjacent fields for the current point in the history of the life of the field , then goes the rapid assessment of stocks of oil and gas and support of the IRT (updating invest Memorandum), and eventually transfers in the project document. The next step is to analyze existing geological and geophysical data and build sector models for the modelling and assessment of IOR.

## References

1. Shatalov I.I., "Monitoring of complex geological models of productive aquifers and surrounding formations on the basis of available and newly incoming information, preparation of exploration programs", «RN-KRASNOYARSKNIPINEFT», Krasnoyarsk, Russia, 2015. (in Russian)

2. Dalacin N. M., Kayachev N.F, Bibik A.S., Shatalov I.I., "Analysis of sites and evaluation of hydrocarbon resources of the Unallocated subsoil Fund and the preparation of the feasibility study the effectiveness of exploration works",«RN-KRASNOYARSKNIPINEFT» Krasnoyarsk, 2015. (in Russian)

3. The materials of seismic records of the previous years.«RN-KRASNOYARSKNIPINEFT», Krasnoyarsk, 2009-2015. (in Russian)

УДК 577.3

# CHEMILUMINESCENCE EMISSION OF SOIL ACTINOMYCETES

**R.Y. Smirnov**
**Scientific supervisor Doctor of Biological Sc. L. S. Tirranen**
**Language consultant Ass. Prof. E. N. Belova**
*Siberian Federal University*

It was found that cultures of higher and lower microscopic fungi exhibit their own chemiluminescence emission, depending on the culturing conditions, which is, apparently, a common feature of fungi. Therefore, provided chemiluminescent radiation from soil actinomycetes is traced, that latter can be considered as an intermediate in the evolution between the highest and lowest microscopic fungi. Literature data on the presence of the chemiluminescent radiation of actinomycetes are not available. The mechanism of radiation is unknown either.

Chemiluminescence emission in the optical region of the spectrum by fruiting body tissues was observed in all studied higher fungi of *Basidiomycota*, and a relatively weak emission was observed in the aerial hyphae of several species of *Ascomycota and Zygomycota*. The analysis of literature data allows to suggest that mushroom chemiluminescence has become the metabolic basis, from which in the course of evolution there came visible bioluminescence of fungi, which creates prerequisites for the study of the chemiluminescence of actinomycetes from soil and to understand the possible molecular mechanism of the chemiluminescent emission from soil actinomyces as actinomyces are structurally close to both bacteria and micromycetes.

The study aims to test the assumption on the ability for chemiluminescence in actinomyces and, if this be true, to study its manifestations depending on culturing conditions.

The study was performed with the bacteria (genus Actinobacteria, division Actinomycetales). All the studied cultures were isolated from soil of Emelyanovskii District of Krasnoyarsk Krai. The Actinomycetales were cultured in media recommended by Nitrusov :( 1Н, 2М, 3К, 4Г, 5КАА, 6Э, 7ОВ, 8ПА). The same nutrient medium with no studied actinomycetales served as a control. The chemiluminescence emission by the studied actinomycetales was detected and its intensity was measured using a Glomax 20/20 luminometer (Promega, United States). The luminometer was calibrated using a Hastings–Weber standard, in which one unit is equal to 2.7 × 103 photons/s. The chemiluminescence emission by each sample was recorded in ten replicates. The isolates were inoculated into the center of Petri dishes 35 mm in diameter, and were then incubated in a constanttemperature cabinet at +26 ± 0.5°C for 21 days. The data were statistically processed according to Lakin using Microsoft Excel and STATISTICA 6.0 software. The significance of differences was estimated using the Student's test. Differences were considered significant at $p \leq 0.05$.

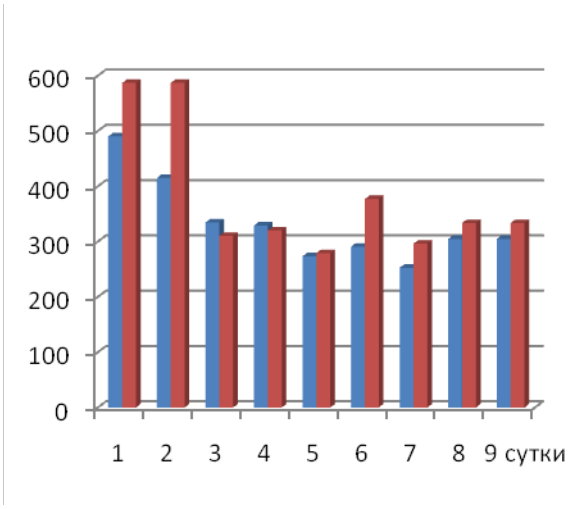


***Fig. 1.Light emission intensity of Actinomycetales in experimental (in different media) cultures (red) and in control (media without yeast)(blue).***

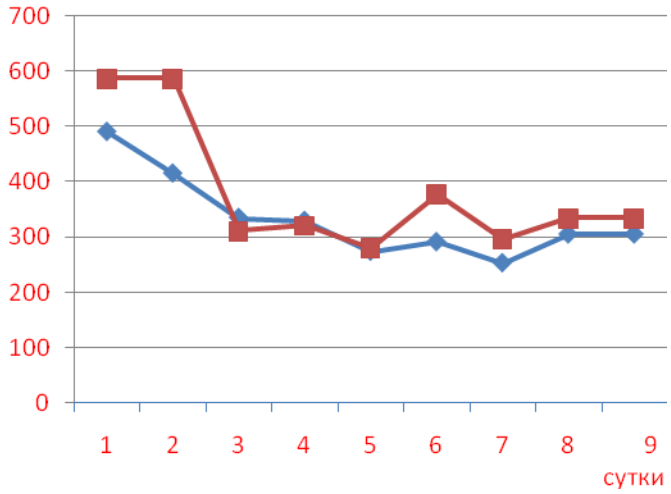


***Fig. 2. Light emission intensity of Actinomycetales during 9 days of culturing in 3Kmedium.***

The results of the study of light emission intensity reliably confirm the dependence of the chemiluminescence emission on the culture medium composition. For example, the intensity of actinomycetes light emission (in six different media) by in the experimental samples was higher in the carbohydrate-containing media.

It is necessary to investigate the source of radiation in fungal cells and the molecular mechanism of this radiation, which can be assumed that the general property of fungi is an evolutionary precursor of intense visible bioluminescence in luminous fungal species.

**References**

1. Nitrusov A.I., Kotova I.B., Microbiology 2006.
2. Lakin, G.F., Biometriya( Biometrics), Moscow : Vysshaya School ,1990.
3. Osamu, S., Bioluminescence Chemical Principles and Methods, Singapore : World Sci., Publ.,2006.
4. Tarusov, B.N., Polivoda, A.I., and Zhuravlev, A.I., Biophysics, 1961, vol. 6, no. 4, pp. 490–492.
5. Taxonomy of fungi, http://meduniver.com/Medical/Microbiology/

UDK 541.49

# STUDY OF THE STRUCTURES AND VIBRATIONAL SPECTRA OF CEFTRIAXONE COMPLEX WITH CR(III)

**Tsyplenkova D.,**
**scientific supervisor candidate of Physics and Mathematics science Kuzubov A.A.**
*Siberian Federal University*

Metal complexes of ceftriaxone have both toxicological and pharmacological properties [1]. While the interaction between ceftriaxone and metal ions can lead to precipitation that results in serious adverse drug events [2], complexes of cephalosporins with Cu(II) are widely studied and used in treatment of diseases such as rheumatoid arthritis [3, 4]. In general, the antibacterial properties of ceftriaxone complexes can increase or decrease relative to pure ceftriaxone [1]. The synthesis of such metal–antibiotic complexes is an important area of medical chemistry [4]. Here, we report the characterization of a Cr(III) complex with ceftriaxone ($H_2$Ceftria) antibiotic. The structure of the new complex was studied using a combination of experimental and computational techniques.

The geometry optimization and harmonic vibrational frequency calculations on the most stable conformers were performed with B3LYP [5] density functional in combination with SBKJC(p,d) basis set [6, 7] augmented with s diffuse functions, as implemented in the GAMESS suite of electronic structure programs [8, 9]. The relativistic effective core potential (ECP) was used for Cr atom. The Grimme's D3 dispersion Ceftriaxone with Cr(III) correction was used in all DFT calculations [10]. All molecular structures were visualized by the ChemCraft program.

Full conformation analysis was carried out earlier [11] using CONFLEX 6.0 program with MMFF94s molecular mechanics force field and Newton–Raphson method for geometry optimization [11]. The results showed the two $Ceftria^{2-}$ dianions in the most stable conformations. Further investigation indicate that the s-cys–s-cys conformer is more energetically favorable than the s-trans–s-cys conformer by 5.9 $kcalM^{-1}$ [11]. The more energetically favorable s-cys–s-cys conformer geometry was used as a ceftriaxone dianion involved in the complex formation. The geometry of the $Ceftria^{2-}$ dianion in that conformation was optimized with B3LYP density functional theory as in earlier investigation [11].

Chromium ion was introduced into the ligand cavity in order to determine the nature of the first coordination sphere. Chromium ion is coordinated by oxygen of the triazine cycle in 6 position, the nitrogen of the amine group of the thiazole ring, and the oxygens of the lactam carbonyl and carboxylate groups. Also the first coordination sphere complemented with $H_2O$ molecule and chloride ion that are coordinated with chromium ion as well. The placement of $H_2O$ molecule and chloride ion near chromium ion has led to the formation of three distinct complexes (figure 1). The complex **I** and **II** differ from each other by the axial spatial location of these groups around the chromium ion. The complex **III** differ from **I** and **II** by the location of $H_2O$ molecule and chloride ion on the one side in reference to Cr atom.

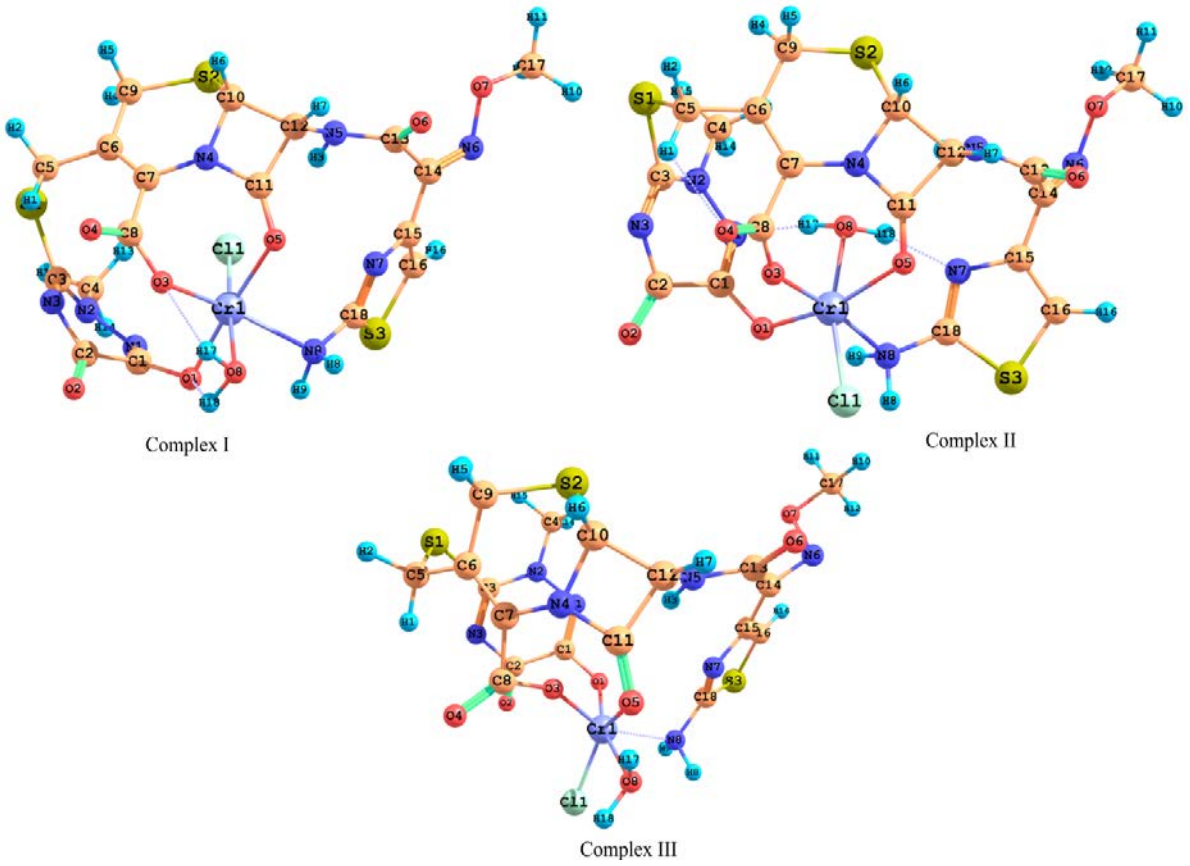


***Figure 1. Structures of ceftriaxone complex with Cr***

According to the B3LYP calculations, the coordination of **I** is 0.5 kcalM$^{-1}$ lower in energy than the coordination of **II**, whereas the coordination of **I** is 19.3 kcalM$^{-1}$ lower in energy than the coordination of **III**. This comparison indicate that coordination structures of **I** and **II** are more energetically favorable and have insignificant difference while complex **III** remains the least stable structure. More detailed comparison of inner coordination sphere of **I** and **II** is shown on Figure 2. Cr(III) ceftriaxone complex represents octahedral geometry.

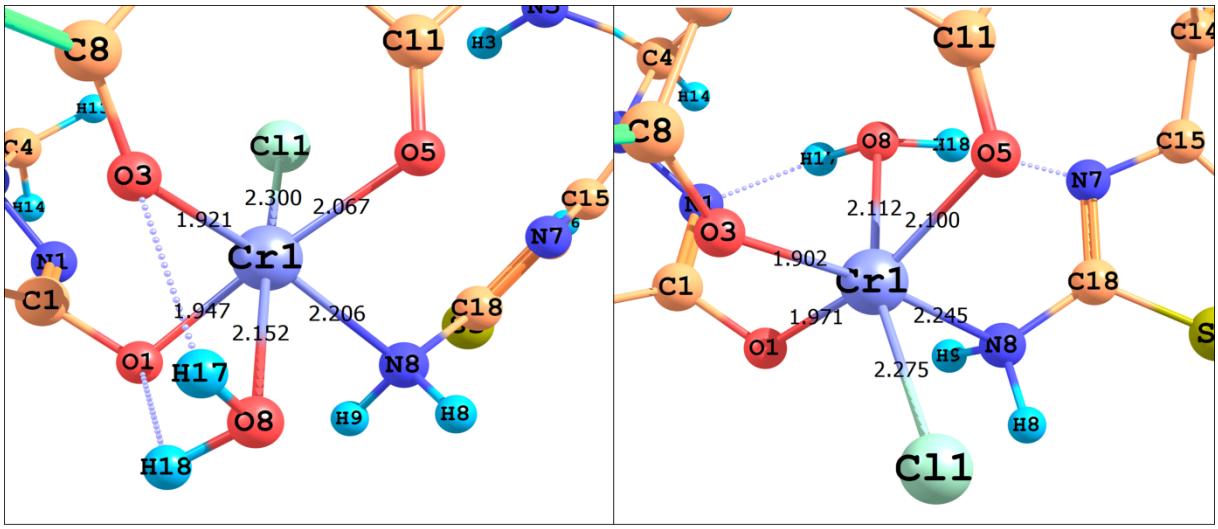


***Figure 2. Inner coordination sphere of I and II with bond lengths in Å***

Table 1. Experimental IR frequencies of Cr(III) with ceftriaxone and calculated B3LYP vibrational frequencies of complex **I** and **II**, $cm^{-1}$

| Exp. frequincies | Complex **I** | | Complex **II** | |
|---|---|---|---|---|
| IR | IR freq. | Functional group | IR freq. | Functional group |
| 1769 | 1762 | ν ($COO^-$) + ν(C=O) lactam + δ($H_2O$) | 1777 | ν(C=O) triazine |
| 1628 | 1622 | δ($H_2O$) + ν ($COO^-$) | 1671 | ν ($COO^-$) + ν(C=O) lactam |
| | | | 1596 | δ(NH2) amine |
| 1537 | 1536 | ν (C=N) triazine + ν(C=O) triazine | 1536 | δ($H_2O$)+ $ν_s$(C=N) triazine + ν(C=O) oxo group |
| 1406 | 1406 | δ(CH2) cephem+ ν(C=N) lactam | 1409 | δ($CH_3$)+ ν(C=O) triazine at position 6 |
| 1380 | 1386 | ν(C–O)-N-N-C triazine+ ν(C=N) triazine + δ($CH_3$) | 1401 | ν(C=N) lactam+ δ($CH_3$) |
| 1351 | 1357 | ν($COO^-$) + ν(C=N) aminothiazole + r(NH2) amine | 1341 | ν($COO^-$)+ ν(C=N) aminothiazole+ δ(CH2) cephem+ δ(CH) lactam |
| 1285 | 1277 | τ(NH2) amine + ω(CH2) cephem | 1281 | δ(CH2) cephem+ ν($COO^-$) |
| 1210 | 1204 | δ(CH) aminothiazole + δ(CH) lactam + ω($CH_3$) | 1206 | δ(CH) lactam+ τ(CH2) cephem |
| 1181 | 1175 | δ(CH) aminothiazole + ω($CH_3$)+ δ(CH) lactam+ r(CH2) cephem | 1172 | δ(CH) aminothiazole + ω($CH_3$)+ δ(CH) lactam + r(CH2) cephem |
| 1102 | 1111 | r(CH3) | 1107 | ω (CH3) |
| 1040 | 1033 | ω(NH2) amine + ω($H_2O$) | 1035 | ω($H_2O$)+ δ(CH) aminothiazole+ ω(NH2) amine |

Table 1 summarizes the calculated vibrational frequencies of the two complexes. The average deviations of the B3LYP frequencies from the experimental values are 5.5 and 8.0 $cm^{-1}$ for **I** and **II**, respectively. The maximum absolute deviations are 9 and 32 $cm^{-1}$ for **I** and **II**, respectively. The broad band in the [Cr(CefTria)($H_2O$)Cl]·4$H_2O$ complex **I** spectrum at 1622 $cm^{-1}$ has the highest intensity and corresponds to bending scissoring vibration of $H_2O$ molecule in the inner sphere. That frequency of complex **I** is very well sorted with experimental 1628 $cm^{-1}$ whereas 1596 $cm^{-1}$ of complex **II** corresponds to another characteristic group and has worse agreement with experimental spectra. Also, it can be the evidence that complex **I** is in structural correspondence with experimentally synthesized [Cr(Ceftria)($H_2O$)Cl]·4$H_2O$ and has $H_2O$ molecule in the inner sphere. However, 1622 $cm^{-1}$ frequency of **I** and 1671 $cm^{-1}$ frequency of **II** has insignificant contribution of $COO^-$ group

vibrations. Moreover, $COO^-$ group vibrations has low intensity in calculated vibrational frequencies of **I** and **II**. All that can be explained by large decrease of O atom charge (table 4) in comparison with ceftriaxone dianion. It was found that all calculated vibrational frequencies of **I** are in better agreement with the experimental IR frequencies than calculated frequencies of **II**. Therefore, the lower energy of **I** and a better match of its calculated vibrational frequencies with experimental IR frequencies indicate that the structure of the synthesized $[Cr(Ceftria)(H_2O)Cl]\cdot 4H_2O$ compound corresponds to **I**.

## Bibliography


1. Anacona J. R., Rodriguez A. Synthesis and antibacterial activity of ceftriaxone metal complexes //Transition metal chemistry. – 2005. – Т. 30. – №. 7. – С. 897-901.
2. Schmutz H. R. et al. In vitro assessment of the formation of ceftriaxone–calcium precipitates in human plasma //Journal of pharmaceutical sciences. – 2011. – Т. 100. – №. 6. – С. 2300-2310.
3. Brown D. H. et al. Antiinflammatory effects of some copper complexes //Journal of medicinal Chemistry. – 1980. – Т. 23. – №. 7. – С. 729-734.
4. Anacona J. R., Patino C. Metalloantibiotics: synthesis and antibacterial activity of ceftazidime metal complexes //Journal of Coordination Chemistry. – 2009. – Т. 62. – №. 4. – С. 613-621.
5. Becke A. D. Density-functional thermochemistry. III. The role of exact exchange //The Journal of chemical physics. – 1993. – Т. 98. – №. 7. – С. 5648-5652.
6. Binkley J. S., Pople J. A., Hehre W. J. Self-consistent molecular orbital methods. 21. Small split-valence basis sets for first-row elements //Journal of the American Chemical Society. – 1980. – Т. 102. – №. 3. – С. 939-947.
7. Stevens W. J., Basch H., Krauss M. Compact effective potentials and efficient shared-exponent basis sets for the first-and second-row atoms //The Journal of chemical physics. – 1984. – Т. 81. – №. 12. – С. 6026-6033.
8. Schmidt M. W. et al. General atomic and molecular electronic structure system //Journal of computational chemistry. – 1993. – Т. 14. – №. 11. – С. 1347-1363.
9. Dykstra C. et al. (ed.). Theory and Applications of Computational Chemistry: the first forty years. – Elsevier, 2011.
10. Grimme S. et al. A consistent and accurate ab initio parametrization of density functional dispersion correction (DFT-D) for the 94 elements H-Pu //The Journal of chemical physics. – 2010. – Т. 132. – №. 15. – С. 154104.
11. Lykhin A. O. et al. A complex of ceftriaxone with Pb (II): synthesis, characterization, and antibacterial activity study //Journal of Coordination Chemistry. – 2014. – Т. 67. – №. 16. – С. 2783-2794.

УДК 546.05

# ANION-EXCHANGE SYNTHESIS OF COPPER FERRITE AND COBALT FERRITE USING ANION EXCHANGER RESIN AB-17-8

**Trofimova T. V.,**
**scientific adviser Professor Saikova S. V.**
*Siberian Federal University*

Ferrites are one of the most popular magnetic materials due to their extensive use in a wide range of applications. They are important in numerous technological applications for example refractory materials, super hard materials, semiconductors, and high-temperature ceramics. It has been widely used for various applications in catalysis, gas sensing, hydrogen production, lithium ion batteries, high density magneto-optic recording devices, magnetic refrigeration and ferro-fluids [1]. In addition, magnetic particles of ferrites used in medicine for image contrast enhancement in magnetic resonance imaging, diagnosis of diseases, targeted delivery of drugs and cancer therapy by magnetic hyperthermia [2].

Ferrites can be prepared by a variety of methods such as solid-state reaction, the mechano-chemical method, sol-gel and co-precipitation method from aqueous solutions. The main disadvantages of solid-state reaction are a continuous grinding of powders and multi-stage heat treatment at high temperatures. The process of the sol-gel synthesis is very long. There are the contact of substances and the formation of compounds take place already at the stage of deposition in the co-precipitation method. However, the product of the synthesis is contaminated particles of the precipitant.

The aim of this work is the selection of optimal conditions for synthesis of copper ferrite and cobalt ferrite by the method of anion-exchange precipitation from solution of a mixture of salts of iron (III), copper (II) and cobalt (II) using strong base anion exchanger resin AB-17-8 in OH-form and the study of composition, structure and properties of the resulting products.

The method of anion-exchange deposition offers several advantages for example the process is done in stationary conditions and obtained particles are homogeneous. Moreover products doesn't contain impurities of the cation and anion of the original salt and therefore don't require multiple operations of washing and cleaning of precipitate. Other advantages of this method are that it doesn't require expensive equipment, the large volume and the duration of the synthesis.

**Experimental**

We used the gel strong-base anion exchanger resin AB-17-8 in OH-form with a grain size of 0.25-0.5 mm. The original anion exchanger resin in the Cl-form is processed through 1M NaOH for 1 h, then 2M NaOH 5-6 times for 1 h. The last portion is maintained during the day. Then, it is washed with water to pH=6-7. The anion exchange resin is dried at a temperature of 60 °C and determined its total exchange capacity through 0.1 M HCl ($C_T$ = 2,28 mmol·eq·$g^{-1}$).

Synthesis technique: 20 g of the water swollen ion exchange resin is brought into contact with a solution of a mixture of salts (16,6 ml of 0.25 M $CuA_2$ or $CoA_2$ and 33,4 ml of 0.25 M $FeA_3$ (where A=$NO_3^-$, $Cl^-$, 1/2 $SO_4^{2-}$)), also containing 5 ml of 0.25 M solution of KSCN or $Na_2C_4H_4O_6$, and 3 h was stirred on the shaker at a speed of 120 $min^{-1}$ at 23 °C. Then the anion exchanger was separated by passing the mixture through a sieve with a hole diameter of 0.16 mm. Centrifugation was carried out for separating the precipitation. The resulting precipitates were dried at 80 °C in and calcined at 950 °C for 3 hours.

The concentration of copper (II), cobalt (II) and iron (III) in solutions were determined by complexometric titration method and atomic absorption spectroscopy.

The structures of the obtained samples were identified using x-ray diffraction analysis (ДРОН-3, CuKα radiation) and scanning electron microscopy (Hitachi TM-1000).

We investigated the change of conductivity of the system copper salt (cobalt, iron) – anion exchange resin over time (conductometer АНИОН 4120) for the purpose of determining the time of complete precipitation of hydroxides of copper (II), cobalt (II) and iron (III). In one case, 5.5 g of the water swollen resin was contacted with 16 ml of 0.25 M $CuCl_2$ ($CoCl_2$); in another case, 16.7 g of the resin was contacted with 34 ml of 0.24 M $FeCl_3$. The electrodes of the conductometer were dipped into the solutions and first, we filmed readings every 1 minute, then after 5 minutes, until a constant conductivity values (for 40-90 min).

**Result and discussion**

The anion - exchange process for the deposition of copper (cobalt) and iron can be described by the following equation:

$$5R\text{-}OH + KA_2 + FeA_3 = 5R\text{-}A + K(OH)_2 + Fe(OH)_3 \quad (1)$$

where K is the cation of initial salt ($Cu^{2+}$, $Co^{2+}$); A is the anion of the initial salt ($NO^{3-}$, $Cl^-$, 1/2 $SO_4^{2-}$); R-OH, R-A are the anion exchanger in –OH and anionic forms, respectively.

The anions of the initial solution are replaced to the OH-ions of the adsorbent and pass into the phase of anion exchanger during the anion-exchange precipitation. The cations of the initial solution are combined in a hydroxide, which leads to lower conductivity of the solution (equation 1). Thus, it is possible to determine the degree of reaction of deposition by reducing the electrical conductivity.

It was found that complete precipitation of copper, cobalt and iron requires a different time. So iron is deposited for 5 min, and the deposition of copper and cobalt requires more than 15 min. This corresponds to values of pH for the start of deposition of cobalt (pH = 6,6), copper (pH = 5,7) and iron (pH = 2) at the used concentrations. Thus, iron is deposited earlier and more fully than copper and cobalt. This leads to disruption of the stoichiometry of the precipitation product.

The activity of $Fe^{3+}$ ions was decreased by injection of the ligand (11 mol. % relative to the sum of metals), which form complexes of medium strength with iron (III) to reduce the deposition rate of iron (tartrate - ions and thiocyanate ions).

In experiments 1 (table 1, 2) potassium thiocyanate was used as the complexing agent. Iron forms complexes of different charge with a thiocyanate-ions ($K_1(Fe(SCN)^{2+})=9.3*10^{-4}$, $K_2([Fe(SCN)_2]^+)=4,7*10^{-5}$, $K_3([Fe(SCN)]_3)=2,3*10^{-5}$, $K_4([Fe(SCN)]^{4-})=3,0*10^{-5}$ [3]), the most stable of which is uncharged $[Fe(SCN)]_3$. The stability of the complexes of copper and cobalt SCN is small. In solutions should prevail positively charged and neutral iron complexes in the indicated concentrations of ligand , however, our research has shown that about 30 % of iron have moved into the phase of anion exchanger. Perhaps this is the result of molecular adsorption of the neutral complex. Thus, the ratio of $Cu^{2+}/Fe^{3+}$ and $Co^{2+}/Fe^{3+}$ in the presence of potassium thiocyanate do not correspond to the stoichiometry. Furthermore, $\alpha Fe_2O_3$, $Fe_3O_4$ phases are present in the products according to x-ray-data in addition to the main phases of $CuFe_2O_4$ and $CoFe_2O_4$, (figure 1a (1), 1b (1)).

In experiments 2-4 (table 1,2) the deposition was carried out on the chlorides, nitrates and sulphates of copper (cobalt) (II) and iron (III) in the presence of tartrate of potassium. Iron forms a number of complexes with tartrate ions ($K_1=3,2*10^{-8}$, $K_2=1.4*10^{-12}$ [3]). In accordance with the distribution chart, iron forms a mixed complex $[Fe(OH)(Tart)^-]$ in the precursor, but the molar fraction of the metal does not exceed 3 % in the phase of anion exchanger at this pH value. It is possible to obtain a precursor containing the impurity ions, with the molar ratio of $Cu^{2+}/Fe^{3+}$ ($Co^{2+}/Fe^{3+}$) close to stoichiometry.

In the presence of tartrate ions, samples of copper ferrite obtained from nitrate, chloride and sulfate salts (table 1, experiments 2, 3 and 4) represent monofase of copper

ferrite after calcination at 950 °C according to XRD analysis (figure 1a). According to scanning electron microscopy (figure 2a), the particles obtained in experiment 4 have octahedral shape and a size of about 1 μm.

Table 1 – Conditions and results of anion-exchange synthesis of copper ferrite ($T_{synth}$ = 23 °C)

| № exp. | Initial salt | n(Cu)/ n(Fe) | $n(SCN^-)$, mmol | $n(C_4H_4O_6^{2-})$, mmol | Elemental analysis of the precursor | | Yield, % | The composition of the products according to the XRD-data (picture 1a) |
|---|---|---|---|---|---|---|---|---|
| | | | | | Molar ratio $Cu^{2+}/Fe^{3+}$ | Anion of salt | | |
| 1 | $Cu(NO_3)_2$ +$Fe(NO_3)_3$ | 0,5 | 1,2 | - | 0,38 | no | 72 | $CuFe_2O_4$, $Fe_2O_3$ |
| 2 | $Cu(NO_3)_2$ +$Fe(NO_3)_3$ | 0,5 | - | 1,2 | 0,46 | traces | 93 | $CuFe_2O_4$ |
| 3 | $CuCl_2$+ $FeCl_3$ | 0,5 | - | 1,2 | 0,46 | no | 86 | $CuFe_2O_4$ |
| 4 | $CuSO_4$+ $Fe_2(SO_4)_3$ | 0,5 | - | 1,2 | 0,47 | no | 98 | $CuFe_2O_4$ |

Table 2 – Conditions and results of anion-exchange synthesis of cobalt ferrite

| № exp. | T, °C | Initial salt | n(Cu)/ n(Fe) | $n(SCN^-)$, mmol | $n(C_4H_4O_6^{2-})$, mmol | Elemental analysis of the precursor | | Yield, % | The composition of the products according to the XRD-data (picture 1b) |
|---|---|---|---|---|---|---|---|---|---|
| | | | | | | Molar ratio $Cu^{2+}/Fe^{3+}$ | Anion of salt | | |
| 1 | 23 | $Co(NO_3)_2$+$Fe(NO_3)_3$ | 0,5 | 1,2 | - | 0,3 | no | 67 | $CoFe_2O_4$ $\alpha Fe_2O_3$, $Fe_3O_4$ |
| 2 | 23 | $Co(NO_3)_2$+$Fe(NO_3)_3$ | 0,5 | - | 1,2 | 0,34 | traces | 85 | $CoFe_2O_4$, $\alpha Fe_2O_3$ |
| 3 | 23 | $CoCl_2$+ $FeCl_3$ | 0,5 | - | 1,2 | 0,38 | no | 83 | $CoFe_2O_4$, $\alpha Fe_2O_3$ |
| 4 | 60 | $CoSO_4$+ $Fe_2(SO_4)_3$ | 0,7 | - | 1,2 | 0,48 | no | 94 | $CoFe_2O_4$, $\alpha Fe_2O_3$ |
| 5 | 60 | $CoSO_4$+ $Fe(NO_3)_3$ | 0,7 | - | 1,2 | 0,46 | traces | 95 | $CoFe_2O_4$ |

In the case of chlorides, nitrates and sulfates as starting salts of cobalt and iron (table 2, experiments 2,3,4), the phase of $\alpha Fe_2O_3$, $Fe_3O_4$ are present in addition to cobalt ferrite

(figure 1b). Only in the case of mixed salts (cobalt sulfate (II) and iron nitrate (III))it was able to obtain a pure phase of cobalt ferrite (figure 1B (a)). According to scanning electron microscopy (figure 2b) particles of $CoFe_2O_4$ obtained as a result of experience 4 have octahedral shape and size from submicron to 3 microns.

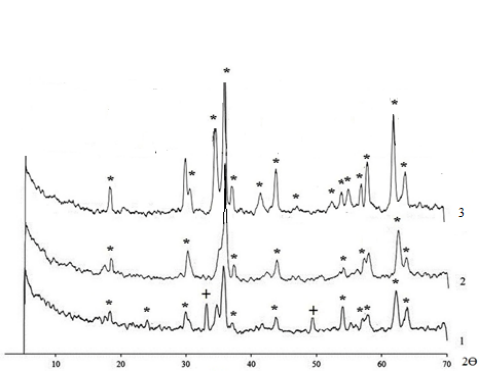

a)

1– exp. 1, 2 – exp. 2-3, 3 – exp. 4

«*»- $CuFe_2O_4$, «+» - $Fe_2O_3$

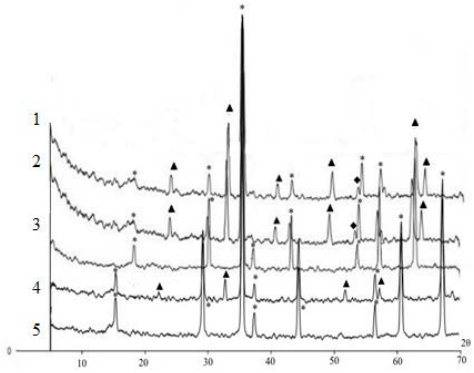

b)

1– exp. 1, 2 – exp. 2, 3 – exp. 4, 4 – exp.3, 5 – exp. 5

«*»- $CoFe_2O_4$, «✓» - $Fe_3O_4$, «▲» - $Fe_2O_3$

***Figure 1 – a) XDR-data for samples of copper ferrite (table 1), b) XDR-data for samples of cobalt ferrite (table 2)***

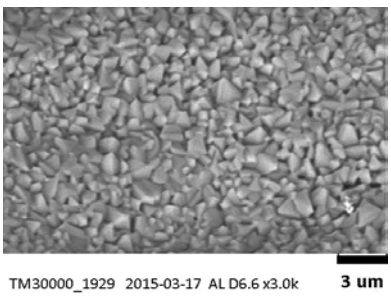


a)

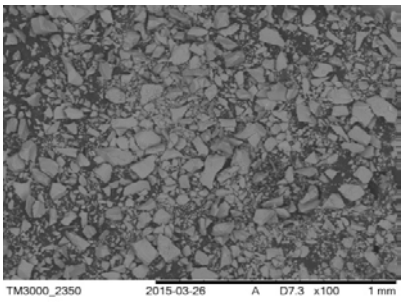


b)

***Figure 2 – a) TEM of particles of CuFe2O4 (experience 2); b) TEM of particles of CoFe2O4 (experience 3)***

The results of measuring the magnetic circular dichroism and magnetization of the synthesized materials indicated their magnetic properties for bulk $CuFe_2O_4$ and $CoFe_2O_4$ [4].

## References


1. Up-scalable synthesis of size-controlled copper ferrite nanocrystals by thermal treatment method / L.B. Zakiyah, E. Saion, N. Soltani, S. Gene // Materials Science in Semiconductor Processing – 2015. - №40. - P. 564-569.
2. Synthesis and characterization of $CuFe_2O_4$ nanoparticles / S.S. Chauhan, C. Ojha, A.K. Shrivastava // International Journal of Theoretical and Applied Sciences - 2009. - №1. - P. 9-11.
3. Lurie, A. A. Handbook of analytical chemistry / A.A. Lurie. – M.: Chemistry, 1971. - 454c. (in Russian)
4. Faraday effect in cubic and tetragonal copper ferrite $CuFe_2O_4$ films—Comparative studies / M. Kucera, V. Kolinsky // Journal of Magnetism and Magnetic Materials - 2007. - №1. - P. 688-692.